NTNU
Norwegian University of
Science and Technology

Dynamic Autonomous Inflow Control Device

Performance prediction and experimental investigation of a specific rate controlled production valve design

Stian Morken Askvik
Ivar Leander Johannessen Sørheim

Petroleum Geoscience and Engineering
Submission date: June 2017
Supervisor: Harald Arne Asheim, IGP

Norwegian University of Science and Technology
Department of Geoscience and Petroleum

Abstract

In conventional completion, control valves either have fixed opening or are dynamically regulated. For Troll wells, inflow control has been implemented by valves where the through-flow regulates the opening. Such valves may have wide applicability once their principles and design are better understood.

The current work considers valve design and measurements to verify the design principles and investigate if additional mechanisms affect the performance. For incompressible flow, the analytic solution presented predicted pressure drop proportional to flow rate in 4th power, proportional to fluid density in 3th power, and inversely proportional to viscosity in 2th power; with proportionality constant depending on valve dimension. Such characteristics imply that viscous oil will flow easier through the valve than less viscous water. This differs fundamentally from those of fixed-opening valves, but was experimentally confirmed for water and high-viscosity oil. The analytical solution enables goal-oriented design of rate-controlled valves.

For gas flow, compressibility effects become important and the analytical solution no longer appropriate. Gas flow was often associated with oscillations, which may contribute to the characteristics measured.

The plane uniformity and surface roughness affect the choking effect and might explain the deviations of some experimental data to the analytic solution.

Preface

This Master Thesis was written as part of the Master of Science in Petroleum Geosciences and Engineering at the Norwegian University of Science and Technology. It was written in cooperation between Stian Morken Askvik and Ivar Leander Johannessen Sørheim. Both of us have a background from petroleum engineering production studies abroad in Australia and NTNU. This master thesis was chosen on the basis that it enabled the combination of product development, practical lab-work and theoretical analysis. This is something that will benefit the both of us as we pursue a career in the petroleum industry.

Most of the lab-testing was done at the department of Geoscience and Petroleum located in Trondheim, Norway. The flow-loop test was made by us because the department did not have any flow-loop facilities available for us to use. This provided us with many challenges that needed to be solved in order to obtain accurate results for the valve tests. The department of Mechanical and Industrial Engineering also contributed with testing of the plane uniformity.

The data when testing was recorded using Labview and analyzed using MATLAB. This provided us with new challenges such as how to organize the data and how to extract the data of interest.

We would first like to thank our thesis advisor Professor Harald Arne Asheim of the department of Geoscience and Petroleum at Norwegian University of Science and Technology. The door to Prof. Asheim office was always open whenever we ran into a trouble spot or had a question about our research or writing. He consistently allowed this paper to be our own work, but steered us in the right direction whenever he thought we needed it.

We would also like to thank the University staff Steffen Wærnes Moen and Noralf Vedvik for providing us with guidance in the lab. The flow-loop facilities would not be of the same quality without these two individuals.

Samandrag

I oljefelt med horisontale brønnar så er det eit kjent problem at vatn og gass kan få tideleg gjennomstrøyming i nokre seksjonar av brønnen, og da oftast i hælen. Rateontrollert produksjon også kalla RCP ventiler har vore installert av Statoil på Trollfeltet for å oppretthalde trykkforskjellen og produksjonsrate etter gjennomstrøyming av vatn eller gass. Det er frå tideligare kjend at RCP-ventilen har ein eigenstyrt strupeeffekt for væsker med lav viskositet. Det er lite publisert arbeide om korleis denne ventilen strupar væsker og kva for parameter som påverkar effekten til ventilen. Det har ikkje vore funn av nokon relevante resultat for denne ventilen som er brukande for å kontrollere forsøka som er publisert. Dette er grunna at dokumentasjonen om denne ventilen blir hemmeligheldt av selskapa.

Måla med denne masteroppgåva er å bekrefte at RCP-ventilen virkar og for å få eit innblikk i korleis den fungerer. For å gjera dette mogeleg har ein analytisk modell vore utvikla og den har blitt kontrollert med eksperimenter. Testinga blei utført med forskjellege væsker, der i blant luft, vatn og olje. Den analytiske modellen simulerte korleis trykk i forhold til straum oppførte seg og dette blei bekrefta av eksperimenta. Da blei og forsøkt å bekrefta om plata inne i ventilen var stabil eller om ventilen ville oppleva vibrasjon. Eksperimenta tyda på at når ventilen strupa trykket så var det ein tydelig vibrasjon. Det blei også sett på om strupeeffekten er avhengig av forskjell i overflatefinhet, jamnhet og størrelse på platene.

Contents

List of Figures

1 Introduction

Horizontal wells may experience an uneven inflow profile from heel to toe. This is due to reservoir heterogeneities, pressure loss in the completion liner and mobility differences in the reservoir. In reservoirs such as Troll with a thin oil column this can lead to early water and/or gas breakthrough reducing the recovery factor. Typically such breakthrough happens near the heel where the pressure drop between reservoir and well is highest. Breakthrough may also be caused by high reservoir permeability and short distance to the gas/oil or water/oil contact. Passive inflow control devices (ICDs) have been applied to delay the unwanted breakthrough. These passive devices increases the differential pressure between the reservoir and the production tubing with a constant choke size. ICDs may be designed to have a pressure drop proportional to the viscosity or to fluid density and velocity squared. Higher viscosity will lead to a higher pressure loss, hence water and gas will flow easier than viscous oil.

Rate Controlled production (RCP) valve is a dynamic Autonomous Inflow Control Device (AICD). The valve was developed by Norsk Hydro to control inflow at Troll.

This thesis considers the working principle of the RCP valve. In order to do this a model based on analytical equations has been proposed and tested using a flow-loop experiment. The tests were done using air, water and hydraulic oil. The tests aim to verify that the analytical based model is able to predict the pressure loss and flow across the valve. It be attempted to verify if the plate inside the RCP valve was stable or if the valve experiences oscillations during choking. It will also be investigated how plane uniformity and surface roughness affects the choking.

2 Rate controlled production at the Troll Field

2.1 RCP valves

Figure 1 shows the original illustration of the RCP AR1 valve. The fluid flow forces the movable plate upwards, thus choking the flow. This design has a chamber underneath the plate to increase the choking for low viscosity fluid.

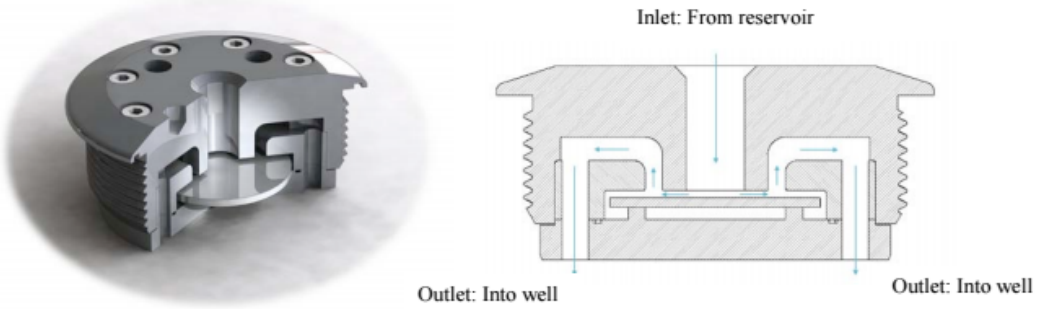

Figure 1: Schematic Design of the old RCP AR1 valve [2]. The fluid flows axially into the valve and then radially over a movable plate.

The RCP AR1 was modified and simplified by Statoil and made smaller to fit the old passive ICD mounts[1]. The valve only consists of three parts; valve body, nozzle and a plate without the pressure chamber underneath the plate as seen in Figure 2[1]. The chamber underneath the valve was deemed irrelevant and was removed. Tungsten carbide was used as material.

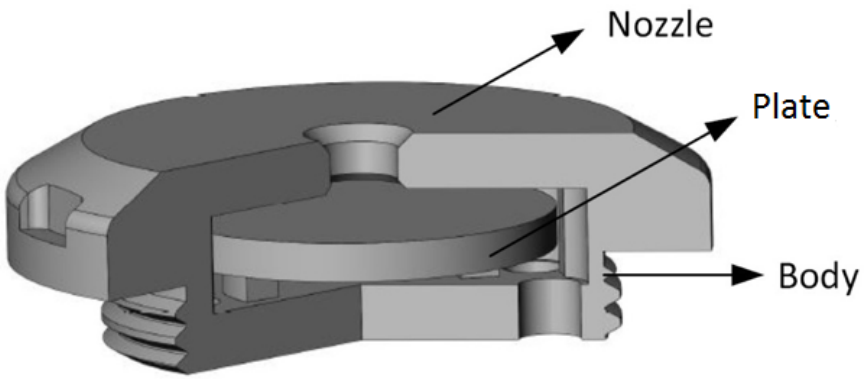

Figure 2: Improved RCP schematic[1]

The valve has been tested with 5ppm of sand in order to measure how much sand it can withstand[1]. The tests were promising and the valve was estimated to outlive the lifespan of Troll[1].

The valve is made in different sizes. With simplified flow paths, the diameter and height is less than half compared to the original. If the valves are too big, the diameter of the production tubing will be affected as the valves are mounted on the inside. This can make interventions difficult as the inside of the production tubing is smaller. [1].

2.2 Production at the Troll Field

The Troll field is located in the northern part of the North Sea, approximately 65 kilometres west of Kollsnes, near Bergen [5]. This field contains an astonishing 40% of total gas reserves on the Norwegian Continental Shelf according to Statoil. It is also one of the largest oil fields in the Norwegian continental shelf according to Statoil.

The oil column on Troll is thin, ranging from 4 to 27 meters[5]. This thin oil column makes producing oil from the Troll field a challenge, both in terms of drilling and completion. This oil column was initially not considered economically viable for development at the Troll field, however, Statoil has broken several technological barriers to enable production of oil at Troll. One of these technologies is the development and invention of the RCP valve.

The wells at Troll are drilled with close to the water-oil contact[1]. The RCP valve enables Statoil to maintain production after breakthrough and makes it possible to have 3 to 5 kilometres horizontal wells on Troll. After 2008 the RCP valves has become standard equipment on Troll with more than 30 wells completed with this technology[1] as of 2016. The new wells drilled on Troll are drilled between old wells where the oil thickness and the water-oil contact can vary. The wells are drilled using geosteering to get the wells as close to the water-oil contact as possible.

In the likely event that a reservoir is heterogeneous, zonal isolation is necessary. High permeability zones will have a higher inflow than the rest of the reservoir. These zones have to be isolated in order to prevent early breakthrough.

If there is no zonal isolation the low-viscosity fluid will flow through the annulus to other inflow regions after breakthrough.

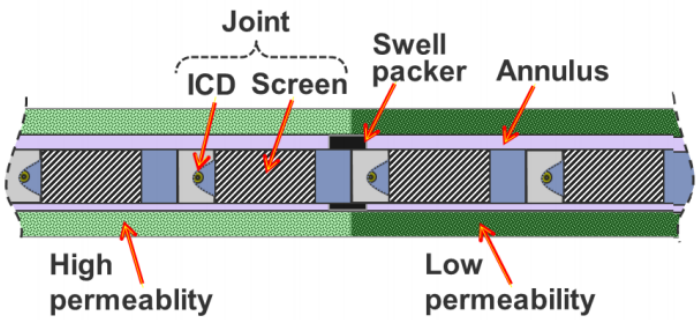

Figure 3: Different producing zones are isolated using packers to avoid annular flow[4]

At Troll all wells are drilled between alternating m-sand and c-sand intervals. The permeability in the c-sands range from 1 to 30 Darcy. The permeability in the m-sand is lower than in the c-sand and can be as low as 0.1 mDarcy[4]. At Troll the wells contain approximately 60-70% c-sands[4]. Therefore due to the different characteristics in the reservoir sands, these zones have to be isolated from each other as seen in Figure 3. Since 2006 the wells at Troll have been installed with between 20-30 swell packers[4].

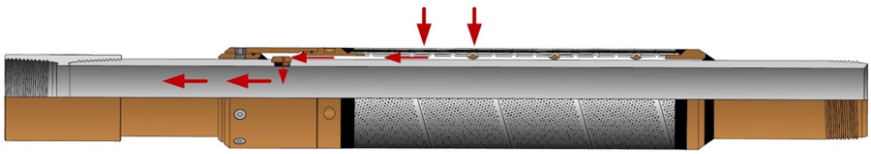

Figure 4: Fluids from the reservoir flow through the sand screen and enters the RCP valve before it enters the production tubing. [1]

The RCP valve is mounted on a pipe joint with a surrounding sand screen as seen in Figure 4. On Troll there has not been detected any sand production as of 2011, sand production is a major concern when utilizing the RCP valve [2]. If the plate is damaged in any way, or a grain of sand is stuck in the valve the choking effect will be compromised. Vibrations may have a devastating effect on such a valve. The vibrations may wear the plate and make it more receptive to cracks. One concern when using this type of valve is fault detection. In a production tubing there may be several hundred RCP valves installed [2].

When installed, it will be a challenge do detect one or several RCPs where the functionality is faulty. Another concern is the lifespan of each value, because functionality of the valves are difficult to monitor long testing and research is crucial.

2.3 RCP valve application

At first Statoil installed the RCP valves in two different wells in the North Sea. The wells were fitted with 1-4 RCP valves per joint, in average 200 - 400 valves per well branch[2].

Light oil reservoir tests and experiments have revealed that the RCP technology reduces gas inflow after breakthrough[2]. In the pilot wells the drawdown was initially 20 bars, and after a few weeks breakthrough occurred[2]. Normally when gas breakthrough occurs the drawdown has to be reduced to 0.5-1 bar. This is to minimize production of unwanted fluids. When the drawdown is lowered the low permeability zones produce less. With RCP technology the gas inflow is reduced and the initial drawdown can be sustained. This leads to higher oil production from low permeability zones. Horizontal wells with RCP technology can be longer and have increased reservoir contact with sustained production.

Laboratory tests done on heavy oil production show that inflow of gas is reduced, but the results also points at reduction in water influx[2].

Figure 5 shows a well. After water breakthrough the drawdown has to be reduced. This will lead to non-uniform inflow profile with coning at the heel. The heavy oil has higher mobility ratio compared to water, it varies from 20 to 100[2]. This means that water will travel faster than oil. Therefore the well will have a significant loss in oil production.

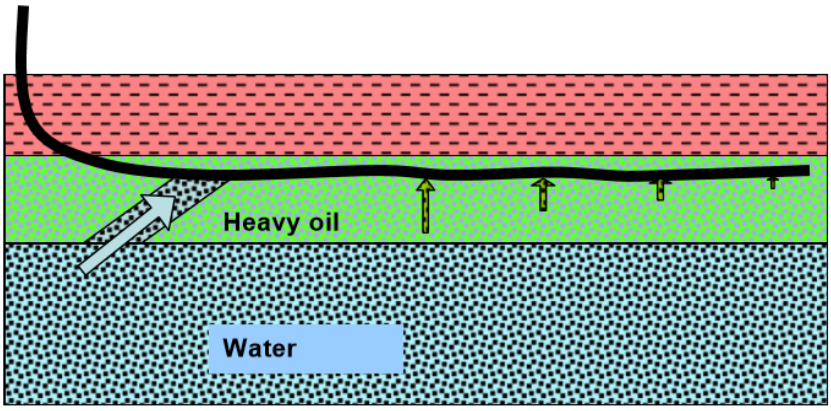

Figure 5: Production of with conventional ICD technology (not RCP valve) [2]

The well producing heavy oil with RCP technology in Figure 6 has a much more uniform inflow profile. After water breakthrough the water production zone will be choked, and oil can be produced from the other zones. The well can produce with the same drawdown as before, without any major decrease in oil production.

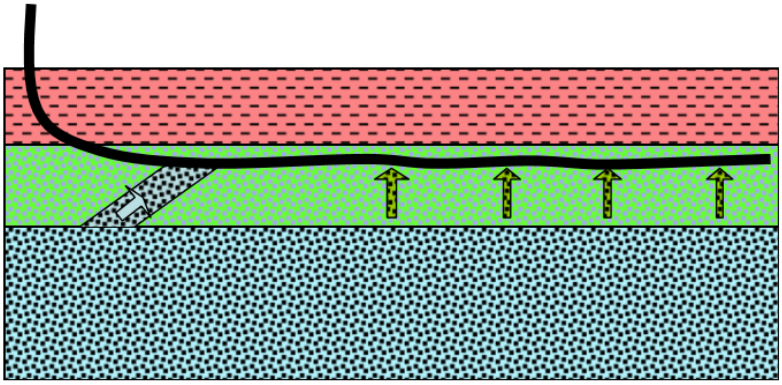

Figure 6: Production of with conventional RCP technology [2]

The first reports on RCP technology is promising in terms of minimizing the effects of breakthrough.

2.4 Results from 3 wells

2.4.1 Troll Well QI-21 BYH

The implementation of the RCP valve on the Troll field has been an important factor in attempting to limit gas coning.

Troll QI-21 BYH was the first well that was completed with RCP valve technology[4]. The objective with this completion was to verify the performance of RCP technology that was determined at Statoil's Multiphase Test Facility in Porsgrunn. This well was completed with two long horizontal branches of 2633 m and 3243 m respectively and with a total of 436 RCP valves[4]. The installation of branch control valves and temperature gauges in the two branches allowed for individual well tests and monitoring individual branches and commingled flow.

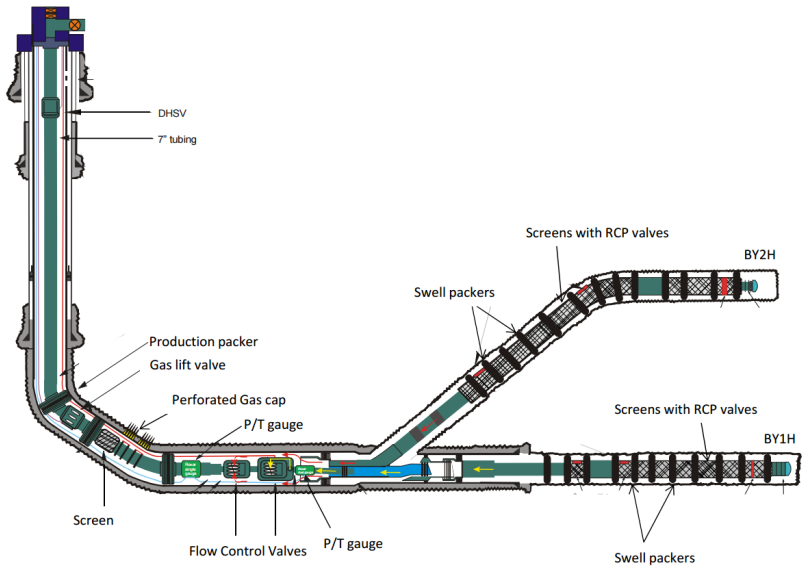

Figure 7: Troll Completion Well Q-21

The installation of pressure gauges enabled Statoil to estimate the pressure drop across the RCP valve. This corresponded to the pressure drop between the reservoir and the tubing, subtracting the pressure drop across the formation. An expression can therefore be determined based on the downhole gauge pressure, reservoir pressure, liquid rate and productivity index.

Based on the well logs the productivity index was higher in branch Y2H, compared to Y1H. Due to this Statoil decided to evaluate the valve characteristics only on branch Y2H. The reason behind this is only stated to be due to higher productivity on this branch, this could lead to confirmation bias.

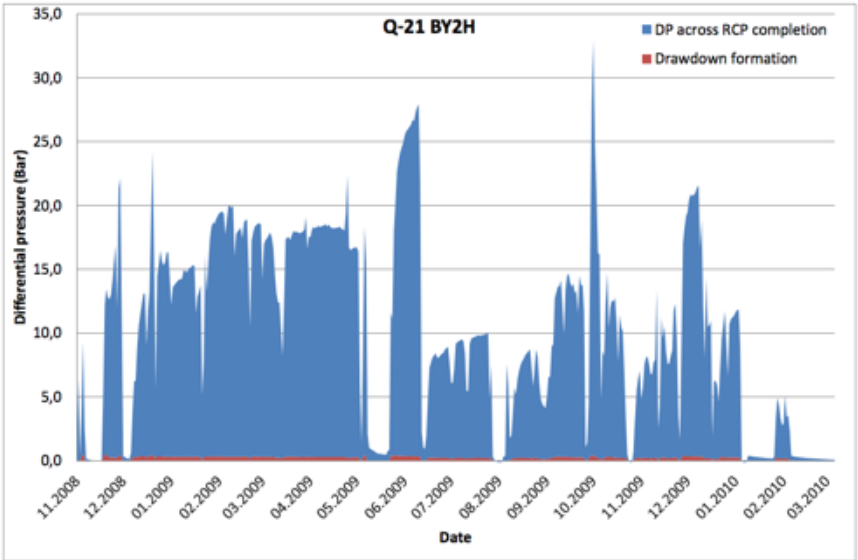

Figure 8: Differential Pressure QI-21 BY2H[4]

The average reservoir depletion on QI-21 BY2H is 2.7 bar per year[4]. In figure 8 the estimated reservoir pressure and the measured tubing pressure is shown. The formation drawdown pressure is based on an estimated liquid production of 25159.24 bbl/d/bar. Figure 8 shows the pressure drop across the RCP valves and the drawdown of the formation, the formation drawdown pressure is small compared to the differential pressure across the RCP completion.

The gas flow rate, oil flow rate and water flow rate is the measured or allocated flow rates at downhole conditions. The RCP valve capacity is found from the respective characteristics of gas, oil and water.

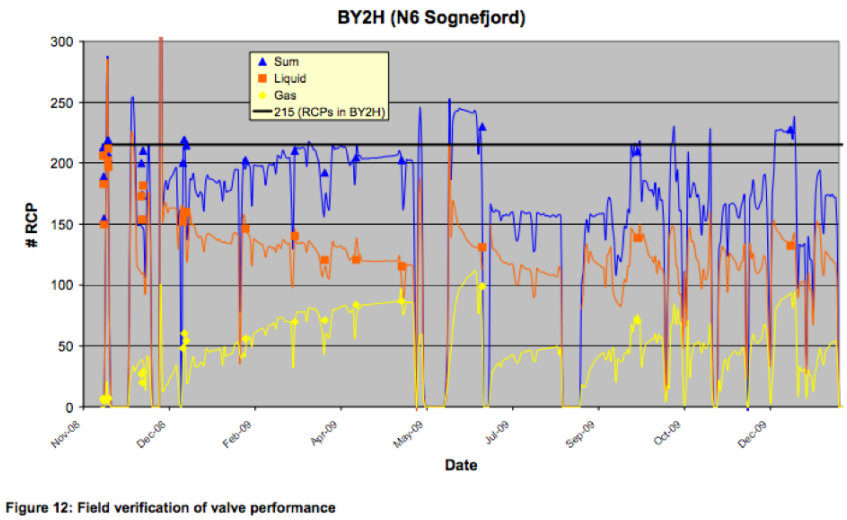

Figure 9: Triangles represent well tests while lines represent allocated rates. This plot was created by Statoil [4]

The minimum number of producing RCP valves found in figure 9 should be lower than the number of RCP valves installed in the branch. The black line in the graph refers to the number of installed valves in the branch(see Figure 9). The number of producing RCP valves is close to the total number of RCP valves in the branch and therefore it is assumed that the whole branch is producing. This was verified with chemical tracers.

Figure 9 indicate that it is possible to produce flow rates through the completion/RCP valve assuming the flow characteristics found at Statoil Multiphase Test Facility in Porsgrunn. The results above also verify that the field characteristics can be according to the flow loop test done at Porsgrunn according by Statoil[4].

However, it must be stated that with the available data from production history it cannot be confirmed that the oil production in QI-21 BYH was any better than one without RCP valves. In this test the water cut and GOR was high, but in the test it was stated that this was most probably due to poor reservoir quality and a thin oil column[4].

2.4.2 Well P-13

The aim of the test at well P-13 was to verify that the RCP completion was better than a conventional well completion with inflow control device(ICD) technology. This was done by drilling to parallel branches through the same reservoir sands, one with conventional (ICD) completion and one with RCP completion.

This was done at welll P-13 BYH on the Troll Field, the figure below shows the well paths. The wells are separated by approximately 191 meters.

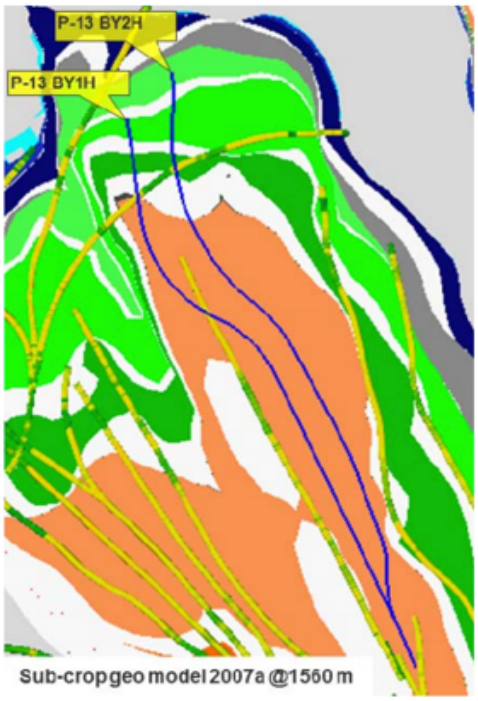

Figure 10: High permeability c-sands are shown in colour while lower permeability m-sands are shown in white[4]

The results of this setup shows a different GOR in the two wells, it is stated by Statoil that this is likely due to the installation of RCP valves in BY2H[4]. It is also evidence to suggest that the RCP valves creates a more continuous inflow and as a result delaying the gas breakthrough and restricting production from zones with a higher GOR compared to other zones.

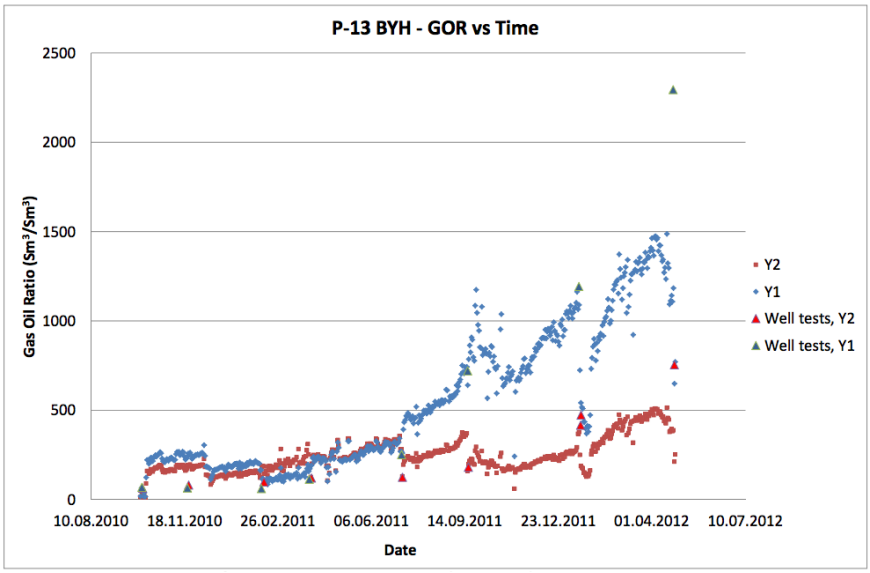

Figure 11: Well P-13 GOR vs. Time. Y2 with RCP completion and Y1 with conventional completion[4]

From Figure 11 it is clear that as the well matures BY1H has a significantly higher GOR than BY2H, the branch completed with RCP valves. It is important to note that the liquid production from each branch is of the same magnitude and that this is not causing the difference in the GOR. The GOR is three times higher in BY1H than BY2H in April 2012, this is a significant difference. By examining Figure 12 it is clear that branch BY2H has produced approximately 20% more oil than BY1H[4].

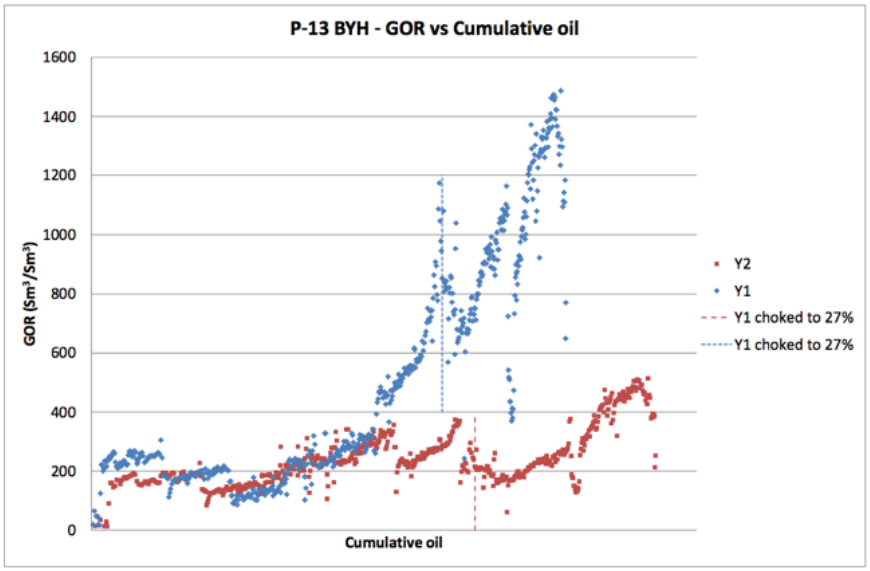

Figure 12: Well P-13 GOR vs. Cumulative oil. Y1 with conventional completion and Y2 with RCP completion[4]

2.4.3 Well P-21

Based on the positive results from both QI-21 BYH and P-13 BYH, Statoil decided to install RCP valves in P-21 BYH[4]. Statoil installed RCP valves in P-21 BYH to increase oil recovery in the area. Figure 13 shows the oil rate and GOR. Statoil states that production in P-21 BYH is high compared to other Troll wells at the time of producing and that in 2012 P-21 BYH was the best producer on the Troll field[4]. This high production rate was maintained for a significantly longer time than is normal for Troll wells.

The GOR in well P-21 BYH is not significant. Other wells with the same GOR development has experienced an increase in water cut and therefore a decline in oil rate. In a 10-month interval well P-21 BYH had produced the same cumulative oil as a typical well at Troll is expected to produce during its whole lifetime[4].

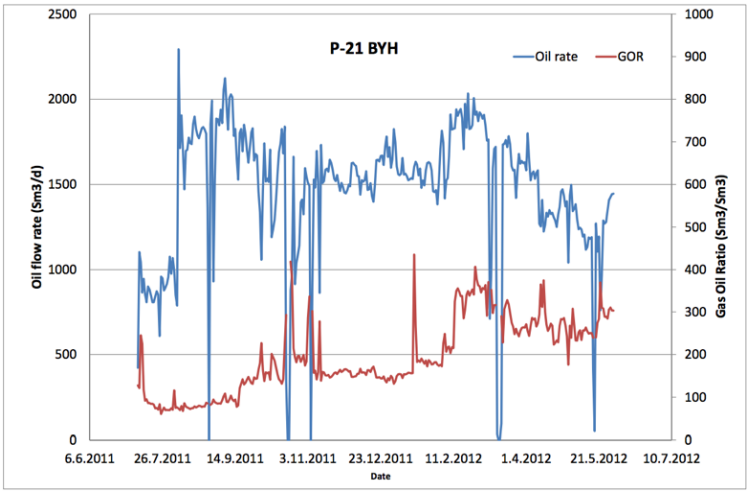

Figure 13: Oil rate and GOR from well P-21 on Troll field

3 Analytical Investigation

3.1 Flow and pressure

When the plate closes, the pressure at the inlet of the valve will increase. This might lead to an oscillating opening and closing of the valve. When the the plate approaches the valve-seat wall conditions and viscosity effects will dominate and stop the valve from closing completely. If this will lead to a stable choking effect or an oscillating effect is difficult to predict.

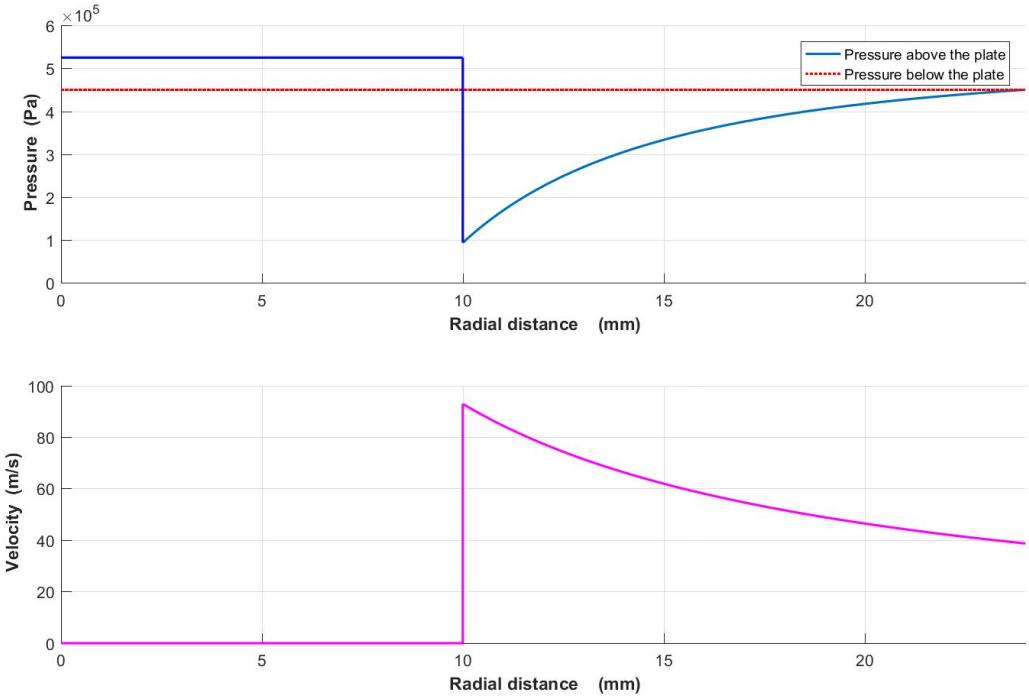

Figure 14: Illustration of the Bernoulli formula in the RCP valve. This example shows a fluid with a density of 100 kg/m^3 and a volumetric flow of 7 l/s

The valve inlet radius is 1 cm and the outer radius of the plate is 2.4 cm. As seen in figure 14 the maximum velocity is approximately 90 m/s, giving a mach number of 0.2647 assuming a sonic velocity of 340 m/s. In fluid dynamics $Ma < 0.25$ is often considered the limit for in-compressible flow.

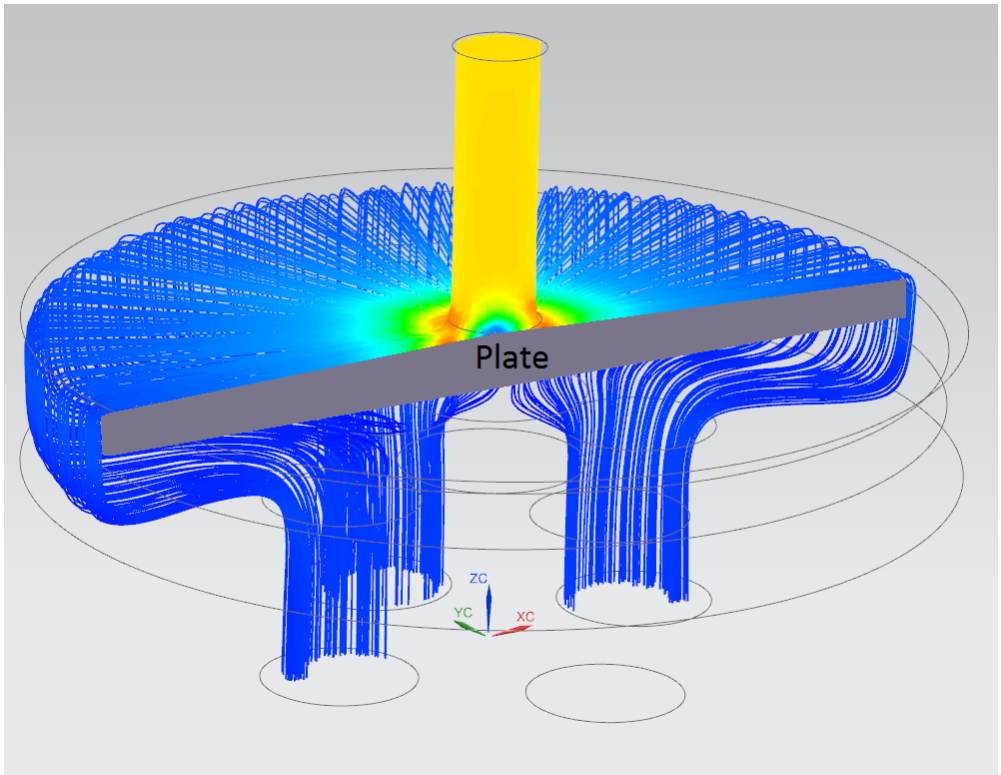

Figure 15: Illustration of the flow area showing velocity streamlines created in Simens-NX11,0

Figure 15 illustrates a simulated flow area of the improved RCP valve seen in Figure 1. The streamlines were calculated in Simens-NX11.0 using the inverted volume. The streamlines show that velocity is highest around the corner of the outlet inside the valve, marked with orange or red. The velocity is higher above the plate than below, marked in blue. This correlates nicely with the theory that the plate will lift. As the speed suddenly increase the pressure will decrease, this will create a lower pressure above the plate and therefore a suction pressure will reduce the flow through the valve. Siemens-NX11.0 was not advanced enough to simulate a movable plate.

3.2 Valve characteristics provided by Statoil

Statoil's multiphase test lab in Porsgrunn confirmed that the RCP valve has a significant potential in horizontal wells when selective choking of fluids is required. The RCP´s effect is displayed in figure 16, and it can be seen that water and gas has a significantly higher choking effect than oil. The curves in figure 16 represent single phase oil, water and gas. As mentioned before, the valve choking effect is dependent on the viscosity of the fluid.

If the reservoir is close to the water-oil contact, the valve will be able to reduce the inflow of water due to the lower viscosity of water[2].

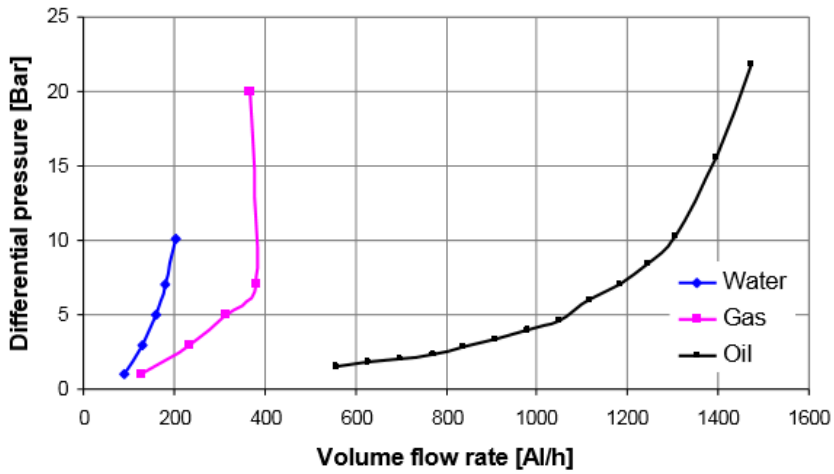

Figure 16: Volume flow of oil (460 cP), water and gas through RCP as a function of differential pressure [2]

The differential pressure above the RCP valve can be expressed by the empirical function f(ρ,μ) developed by Statoil:

$$f(\rho,\mu) = \left(\frac{\rho_{mix}^2}{\rho_{cal}}\right) * \left(\frac{\mu_{cal}}{\mu_{mix}}\right)^y * (a_{RCP}) * q^x \tag{1}$$

a_{RCP}, x and y are user input parameters that are based on the RCP valve, q is the local mixture volumetric flow rate. User inputs μ_{cal} and ρ_{cal} are calibration viscosity and density. μ_{mix} and ρ_{mix} are based on the following equations:

$$\rho_{mix} = \alpha_{oil}^a \rho_{oil} + \alpha_{gas}^b \rho_{gas} + \alpha_{water}^c \rho_{water} \tag{2}$$

$$\mu_{mix} = \alpha_{oil}^d \mu_{oil} + \alpha_{gas}^e \mu_{gas} + \alpha_{water}^f \mu_{water} \tag{3}$$

a, b, c, d, e, f have been implemented into the mixture equations to aid better description of the mixture properties at multiphase conditions.

The empirical equation 1 is given by Statoil[1]. The formula is used in combination with dynamic reservoir simulations to calculate the differential pressure, and to calculate how many valves is needed in the tubing.

3.3 Analytical Solution of RCP valve

A solution devised by Asheim assume incompressible fluid and when the flow is constant the plate is in a stable position[1]. After some simplifications the pressure loss across the valve can be expressed as:

$$\Delta P = \frac{\rho^3}{\mu^2} C_4 Q^4 - \rho C_2 Q^2 \tag{4}$$

C_4 and C_2 are design dependant and involve parameters: r_e, r_i and E (the efficiency). The radius is given in milimeter, density in kg/m^3, viscosity in centi-poise and the flow in $liter/s$. The constants C_4 and C_2 can be determined with:

$$C_4 = 357 \frac{1}{r_i^6} \left(\frac{1}{4} \frac{r_i^2}{r_e^2} (1 - E)) + f_d \ln(\frac{r_e}{r_i}) f_d^2 \right) \tag{5}$$

$$C_2 = \frac{2.5}{r_i^4} \tag{6}$$

Where:

$$f_d = \frac{\ln(r_e/r_i) - 0.5(1 - E))}{(r_e/r_i)^2 - 1} \tag{7}$$

It can be seen from equation 4 that the pressure loss across the valve will be approximately in the fourth order: $\Delta P \propto Q^4$. In comparison the pressure loss across ordinary nozzles are in the second order: $\Delta P \propto Q^2$. The dynamical Bernoulli valve should therefore be less affected by pressure variations.

According to equation 4 the pressure loss is proportional to density cubed and inversely proportional to viscosity squared: $\Delta P \propto \frac{\rho^3}{\mu^2}$. This means that oil (with a higher viscosity) will flow more easily through the valve than a lower viscosity fluid such as water (if one assumes that the viscosity difference will dominate compared to a slightly smaller density). In comparison the pressure loss across an ordinary nozzle is proportional to the density: $\Delta P \propto \rho$, assuming turbulent flow unaffected by density.

Gas has a much lower viscosity than both oil and water and therefore according to equation 4 it will have a much higher 'resistance to flow'.

[1]Obtained through personal communication with Prof. Harald Arne Asheim[11]

This is a rough estimate due to the fact that gas is not in-compressible and some gas principles are not taken into account in this equation.

With this analytical approach it is possible to design a valve with needed characteristics due to the parameters C_4 and C_2. It is seen from equation 4 that C_4 will likely dominate the characteristics.

Based on the equations above a Matlab script was made in order to predict the choking effect of water and oil flowing through the valve. This model is based on the same assumptions as the equations above and there are several parameters that are not taken into account such as uniformity of the plate and surface roughness. These are mostly design parameters that are difficult to implement into Matlab.

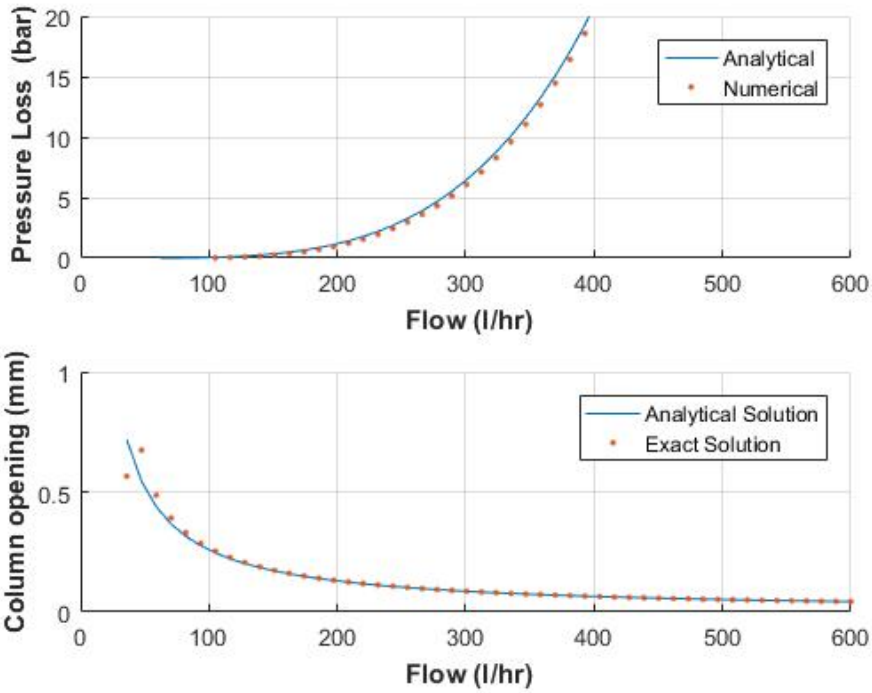

Figure 17: Predicting performance of RCP valve. Valve-seat of 40 mm and plate radius of 1.5 mm. Inlet pressure of 6 barg.

4 Experimental Investigation

A simple equation has been proposed and it will be tested using a flow-loop. The RCP is expected to have a selective choking effect based on the viscosity, the plate plane uniformity, plate size and surface roughness.

4.1 Valve design and manufacturing

4.1.1 The old RCP Valve

The first RCP valve was developed and designed from Hydro's (now Statoil) RCP valve patent found at the Norwegian Industrial Property Office. The valve was made by computer aided design in Siemens NX11.0. To avoid corrosion the valve was manufactured in stainless steel. 3D illustrations and the technical drawings of the different parts can be found in appendix A.2.

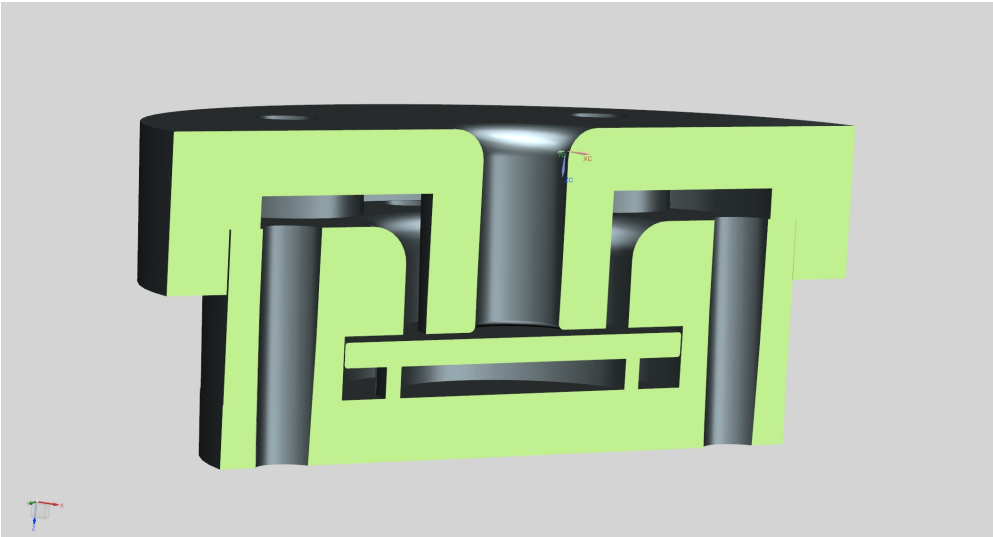

Figure 18: 3D assembly of the old RCP valve. It shows a design that was difficult to seal.

Figure 18 illustrates the 3D assembly of the RCP valve. There were a lot of challenges associated with this RCP design. First of all the valve proved difficult to seal due to the complexity of the four separate parts. After several attempts to seal the valve a custom-made gasket was used. The gaskets made it impossible to correctly measure the distance 'h' between the plate and valve-seat. Therefore a new design was tested.

4.1.2 The modified RCP valve

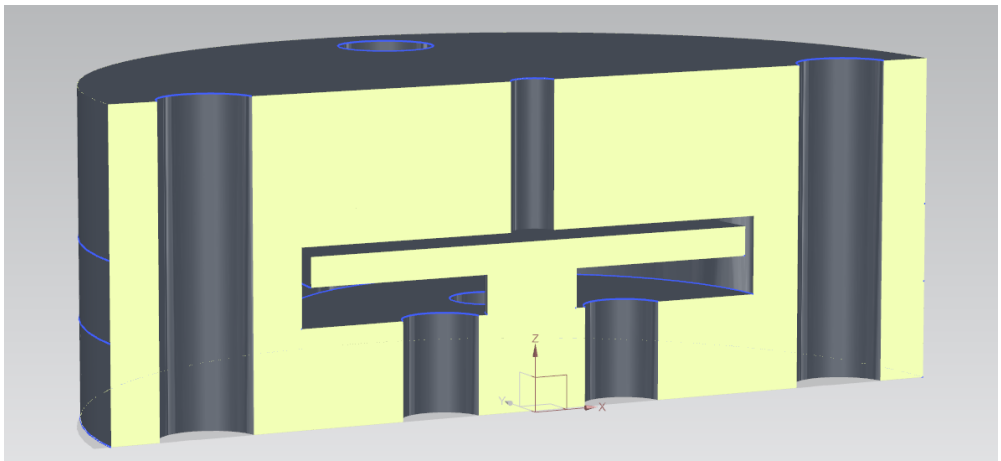

Figure 19: 3D Assembly of the improved RCP valve. It shows a more simple flowpath than the old design.

Figure 19 illustrates the improved valve based on Statoil's RCP valve designed by Halvorsen et. al. as seen in the paper from 2016[1]. This valve consists only of three parts and was significantly easier to manufacture and seal. Three different valves were made with chambers of Ø50mm, Ø40mm and Ø30mm in order to tests how the plate radius affected the choking effect. With this new design the contact area between the plate and the valve was maximized, which could lead to a higher suction pressure of the plate and a higher differential pressure. This design saved production time and material because it was possible to make four different top parts and only one bottom part. The size of the valve doesn't matter in this experiment, but for production in a real reservoir the valve should be as small as possible. The technical drawings and the 3D illustrations can be found in appendix A.3.

4.1.3 Plane uniformity

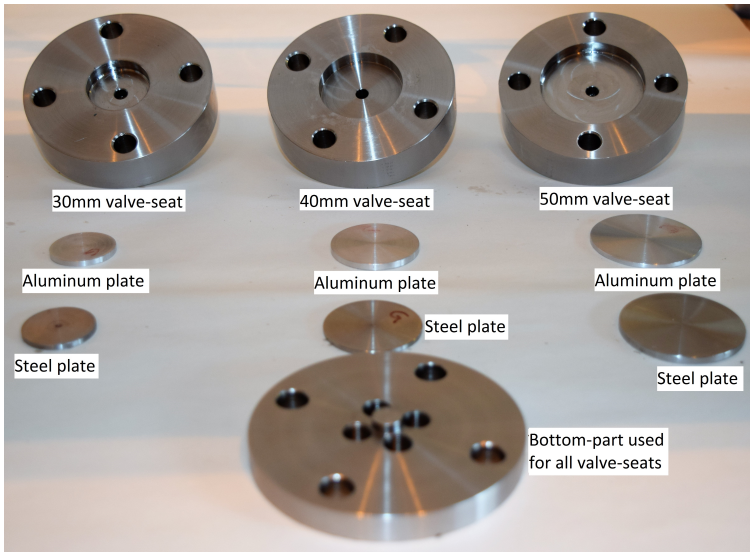

Figure 20: Picture of all three valves and corresponding plates in aluminum and stainless steel. The valve bottom-part is seen at the bottom.

Figure 20 shows all the parts of the valve, valve-seat at the top, the plates in the middle and the valve outlet at the bottom. It was difficult to get the exactly the same features on each plate. The plates were made in a manual lathe. This meant that thickness was set manually which can lead to differences. As thickness varies, forces on the turned plate changes during cutting. This lead to differences in surface roughness, weight due to volume changes and mechanical tension. Inner mechanical tension was a result of a cutting process where local heat affected the material. This combined with a relatively thin plate compared to the diameter may have lead to major inner mechanical tension. Unrelieved tension could make the plate uneven or twisted. Another concern during the turning process was that the plate was too thin. As the plate was cut the heat and the axial forces (which can accrue) would push the plate, making it uneven and almost spherical.

Due to the limitations of equipment and resources the plates were made in a simple manner where mechanical tension was not properly dealt with. This was due to time constraints and poor knowledge. The uniformity measurements will reveal if the plates and valves were affected by mechanical tension. Different surface roughness was wanted in order to test if there was a clear correlation between surface roughness and choking.

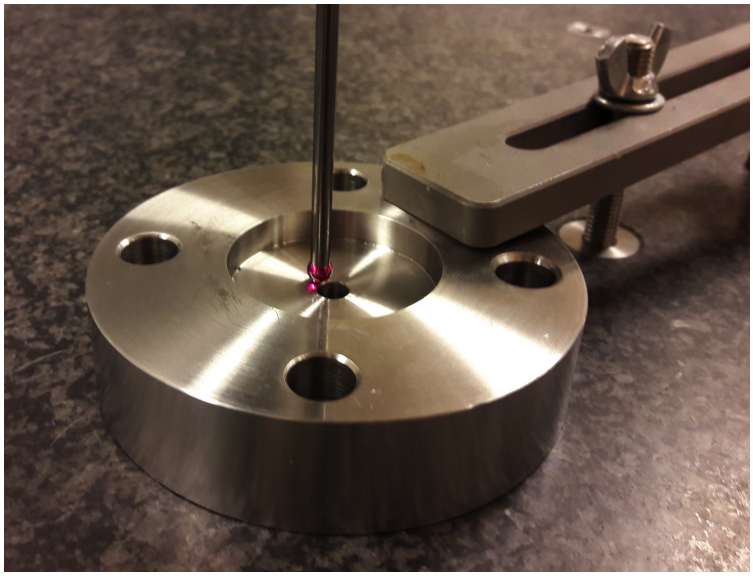

Figure 21: Picture of the measurement probe in the Leitz pmm-c inside the valve-seat.

The measurements of the parts were done in a Leitz pmm-c in order to test the plane uniformity. Different points on the plate/valve was measured. Figure 21 shows how the plane uniformity was measured inside the 40mm valve-seat. The distance between the valve-seat and the plate can vary depending on the plane uniformity of both the plate and the valve. If the plate and the valve-seat had uneven planes that doesn't match the choking effect might be compromised.

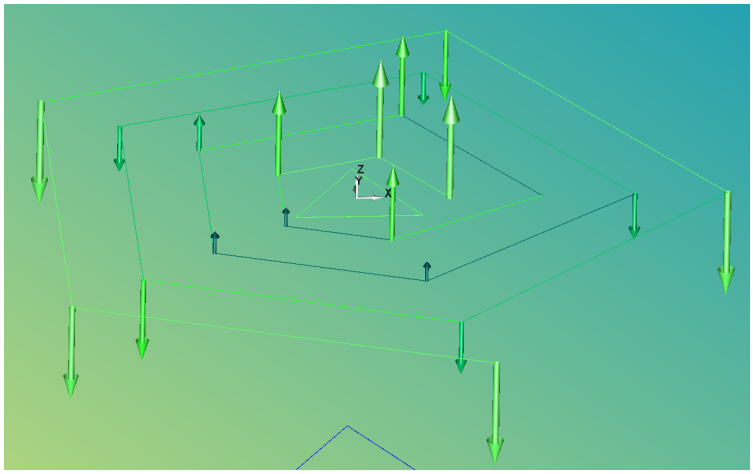

Figure 22: Uniformity measurement of the 40 mm valve-seat. The measurement shows that the valve-seat had a slightly convex shape with a uniformity measurement of 0.004 mm.

Figure 22 shows the plane uniformity of the 40mm valve. The valve had a uniformity measurement of 0.004 mm, this is very low compared to the other plates/the other valves. The 40 mm valve was made in a lathe.

$$MPE = \pm \left(0.6 + Lenght\,(mm)\,/600\right)\mu m \tag{8}$$

The maximum permissible error for the Leitz pmm-c was estimated using equation 8. The error was very small compared to the measurements taken and was therefore considered to be negligible.

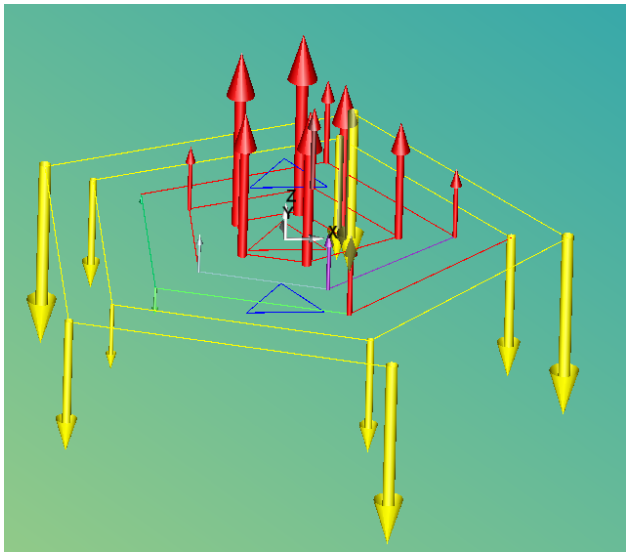

Figure 23: Uniformity measurement of the 50mm valve-seat with a value of 0.029 mm. It shows that the 50 mm valve-seat had a convex shape. The uniformity is larger than in the 40 mm valve-seat.

Figure 23 shows plane uniformity of the 50mm valve, as seen in the figure the valve was convex and had a uniformity measurement of 0.029 mm. This deviation may affect the flow results. The 50mm valve was milled and not made in a lathe such as the 40 mm valve. The explanation for this convex shape may be that the milling machine was old and worn.

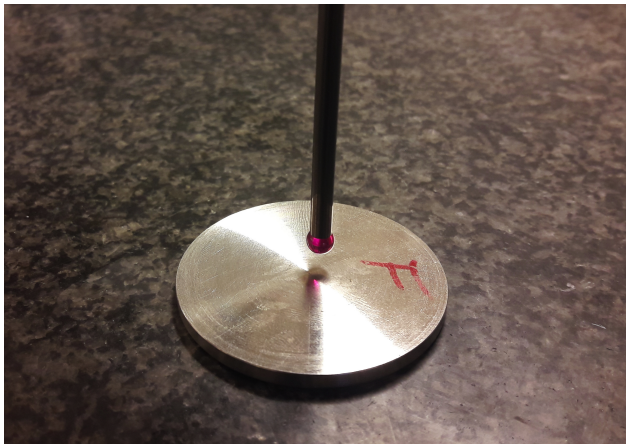

Figure 24: Picture of how the uniformity measurement was done on the plates in the Leitz pmm-c.

Surface roughness and plane uniformity was measured for all the plates on both sides. The surface roughness was measured using a Elcometer 7060/4. The results clearly show a smoother surface on aluminum plates than on the stainless steel plates. Surface roughness and plane uniformity measurements can be found in A.1.

4.2 Experimental setup

4.2.1 Flow equipment

When starting the experiment the first concern was to find a pressure source. Several pumps were tested, but none could deliver the required pressure. The pumps on hand also had an uneven pulse problem, these pulses could disrupt the plate and affect the results. Water pressure from the wall socket was used because it delivered the most stable pressure. The disadvantage of the water source was that it had a maximum pressure of 7 bara.

As the pumps were not an option it was decided to use a pressure supported tank to deliver oil pressure. The oil pressure was supported by water from the wall socket. A 120 litre pressure proof tank was installed with 40 litres of oil. 40 liters was enough to conduct the experiment, because the used oil could be returned to the pressure tank after a valve test. The remaining 80 litres of water was a buffer to make it easier to dispose the water. As emulsions started the bled water was dumped in a disposal tank instead.

For gas testing the air socket from the work-shop was used. This pressure was stable and was able to deliver 7 bara. The pressure tank was disconnected when testing with gas.

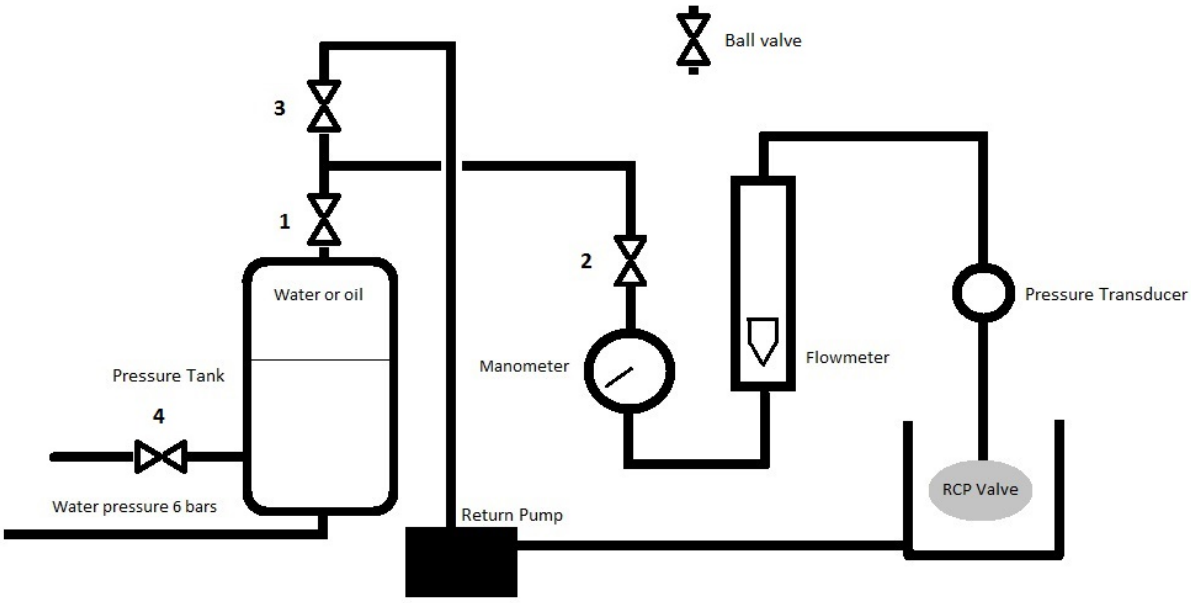

Figure 25: Flow Diagram of the flow-loop testing facilities. The flow-loop was modified when testing gas. The gas from the workshop was connected to ball valve 2.

Figure 25 is an illustration of the experimental setup for oil and water. All parts were connected using rubber tubes with hose clamps. The hose clamps were certified for a 10 bar pressure system. Hose brasses were used between the equipment and hoses, they were sealed with thread sealing tape. This was done to secure a steady pressure and to avoid leakage.

4.2.2 Computer program

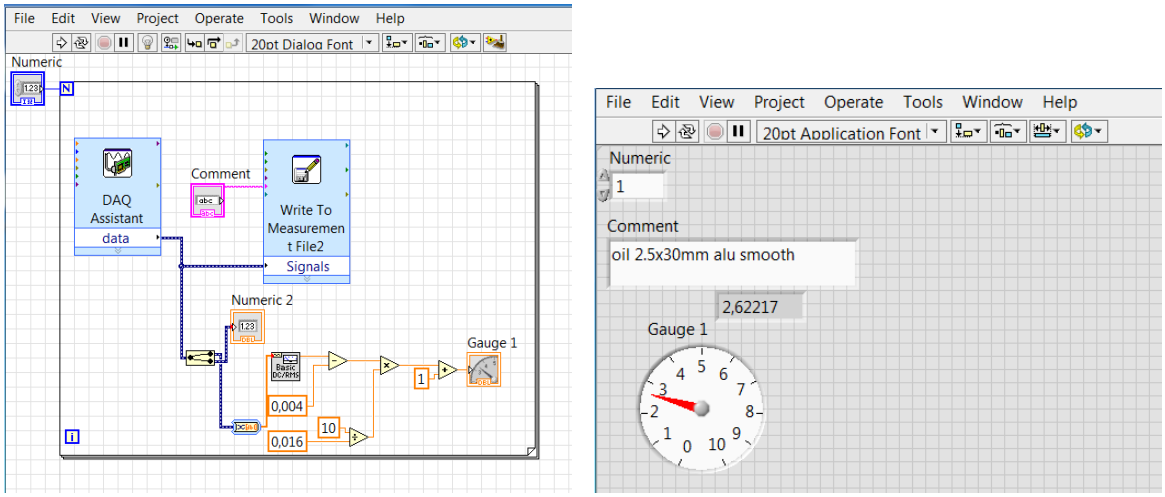

(a) Block diagram for Labview setup (b) Labview front panel

Figure 26: Labview program used to measure flow and frequency

In Labview, DAQ assistant was used to read the pressure transducer(Druck Gauge for liquid sensor). The vibrations in the plate was estimated with high frequency (1000 samples per second) samples, giving a Nyquist frequency of 500 Hz. This theory says that the sampling rate needs to be twice or higher compared to the expected measured frequency.

The fast Fourier transform algorithm was used to analyze the pressure pulses to get a frequency spectrum plot.

4.2.3 Calibration

The Fisher & Porter flowmeter was calibrated for the different fluids. When testing air, a table was used as it was difficult to measure the air flow. Tables provided for the flowmeter stated that 100% flow was approximately 17.3 m^3/h [9]. For water and oil the calibration was done experimentally. Flow was measured at different rates and volume flow and time was noted. This provided the correct volume rate for both water and oil.

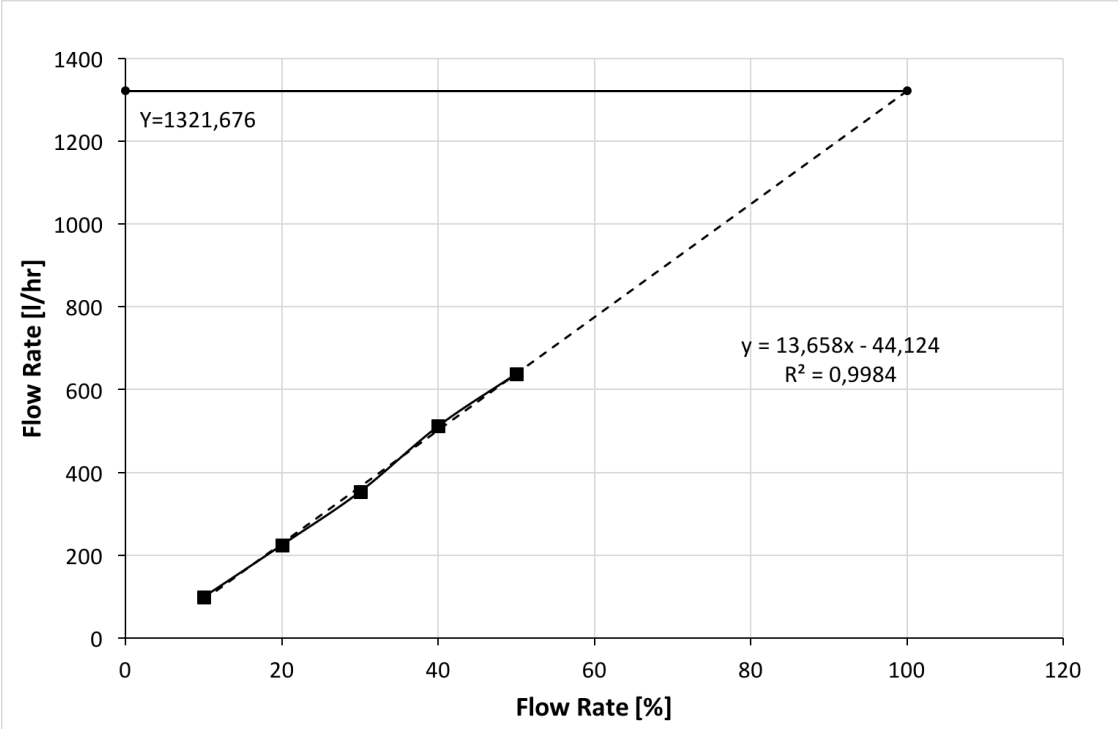

Figure 27: Oil-rate calibration results. It shows that the 100 % mark on the flowmeter corresponds to a flow of 1321.676 l/hr. This relationship is linear.

As seen on Figure 27 the oilrate at 100% was 1321,676 l/hr. The available rates were measured and a linear regression was used to find the 100% point. The flowmeter used for oil was not the same used for air and water. Oil testing required a flowmeter with a higher capacity than water.

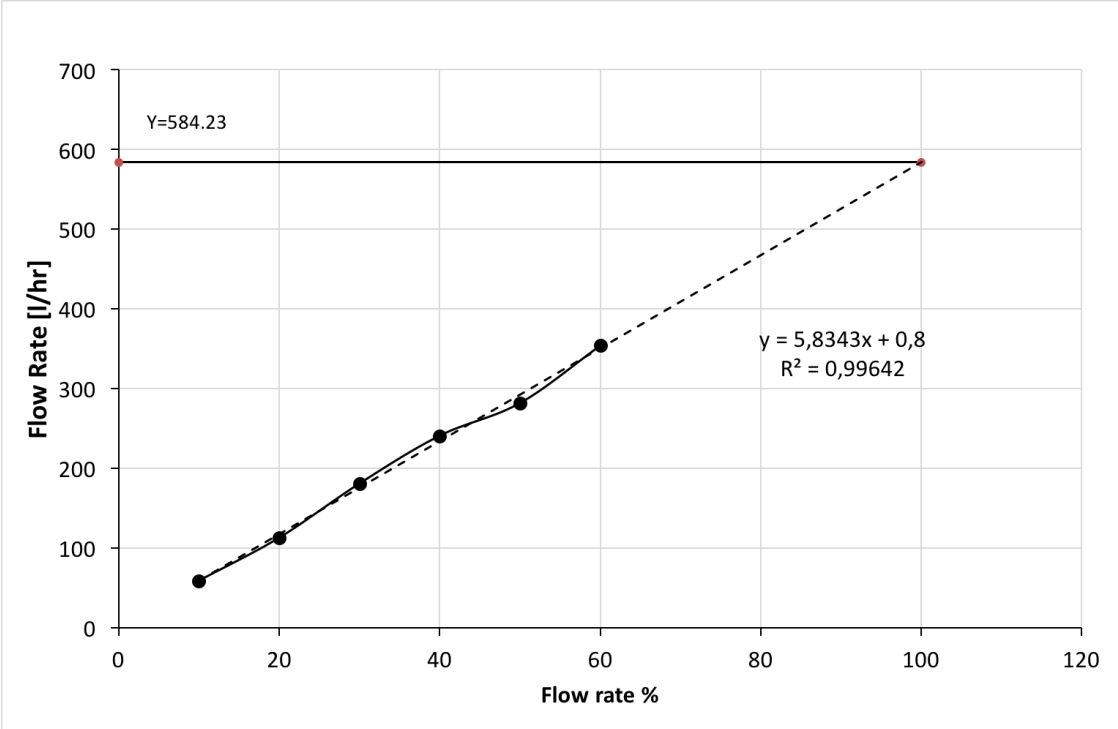

Figure 28: Water-rate calibration results. It shows that the 100 % mark on the flowmeter corresponds to a flow of 584.23 l/hr. This relationship is linear.

As seen on Figure 28 the 100% rate for this flowmeter with water was 584,23 l/hr.

The pressure transducer (Druck Gauge for fluid pressure sensor) was calibrated using the atmospheric pressure and a tested pressure. The analog pressure manometer was used to read the higher pressure. The pressure transducer delivered a linear reading in milliampere. Therefore two measure-points was enough to make a linear extrapolation. The pressure transducer was mounted before the valve inlet in order to measure both the pressure across the valve and the pressure vibrations in the valve.

4.3 Experimental procedure

When testing the three different fluids almost the same equipment was used. The air socket was connected directly to the ball valve number two, seen in Figure 25. The outlet pressure of the valve was one bara because RCP valve was open to atmosphere.

For water and oil testing a pressure tank was used. The outlet pressure for oil and water was also one bara as the valve released the fluid into an open bucket.

After testing, the fluid was pumped back to the pressure tank. To be able to pump something back into the tank, ball valve number four was mounted. This valve bled the tank pressure. With water the excess fluid was disposed the sink, and for oil testing the excess oil/water emulsion was disposed in a tank.

The procedure:

- Choose a plate and assemble the valve
- Fasten the valve to the tube with hose clamp
- Put the valve in the bucket
- Close all ball valves
- Apply pressure to the system
- Open ball valve number one (for oil and water testing)
- Open ball valve two to wanted flow (read from Fisher & Porter Flowmeter)
- If the flow doesn't change use the manometer (CVK Bar Manonmeter) for support.
- Run Labview program and acquire pressure and frequency readings.
- Open ball valve two some more and repeat this sequence for every wanted flow/pressure.
- Close all ball valves

  Do not apply for air testing:

- Close water socket pressure
- Open ball valve 4 to bleed the pressure tank
- Open ball valve one and two
- Pump water/oil to the pressure tank.
- Close all ball valves
- Remove and dismantle the valve

Using a Brookfield viscometer DV-2 Pro the viscosity was measured. This was necessary because the oil was in an emulsion with water and the viscosity was not known at the measuring temperature. The viscosity was measured to be 64 Cp at 15 °C.

The oil emulsion density was measured with a pycnometer. The density was calculated to 857 kg/m^3.

5 Results

5.1 Water Flow

5.1.1 Valve Performance

Figure 29 shows the pressure loss across the valve when flowing water. The test was done using a valve size of 40 mm with a 2 mm thick aluminum plate. The choking effect starts after a flow of approximately 220 l/hr was reached, after this the pressure increases exponentially. When the plate was choking a clear 'noise' was observed that increased proportionally to the differential pressure across the valve. Both the analytical model and the experimental result shows an exponential choking effect. However, the experimental data has a more exponential(steeper curve) choking effect than the model data. The model data given in Figure 29 is taken from from the model presented in Chapter 3.3.

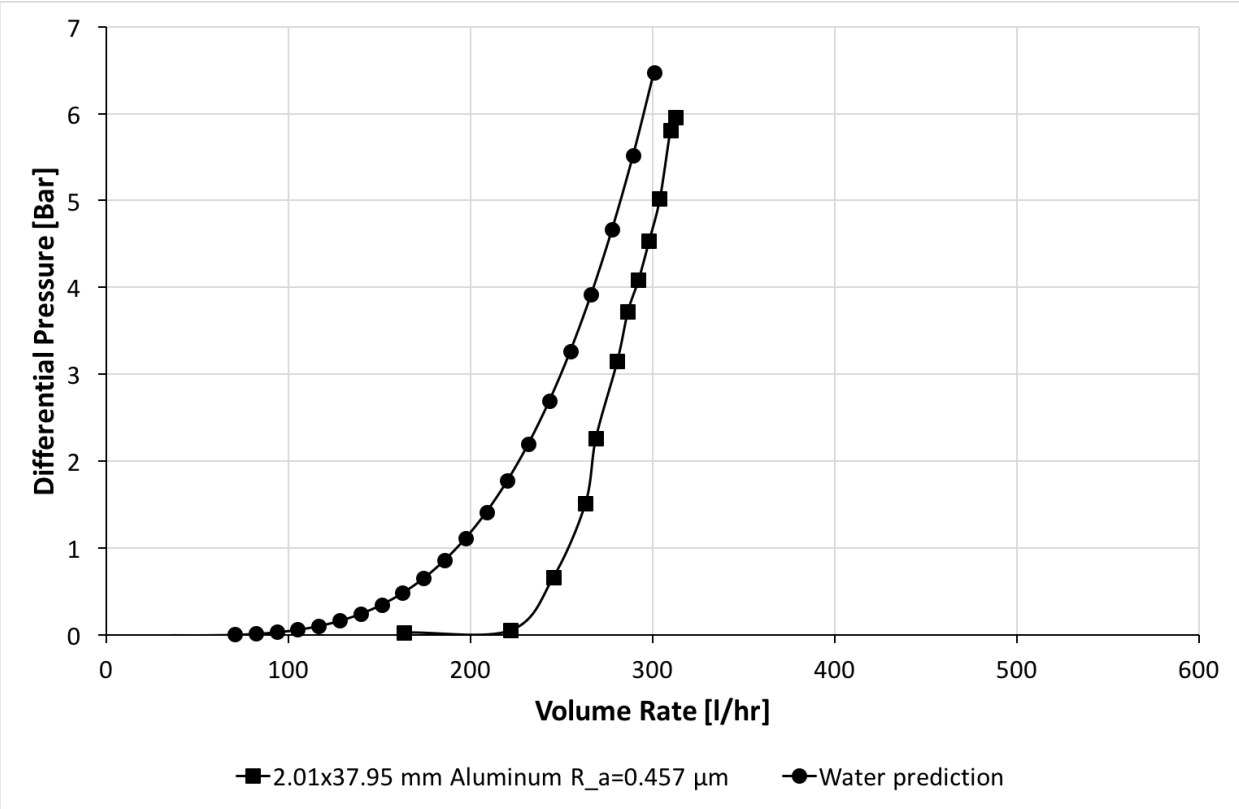

Figure 29: Performance results from analytical method and experiments. The plate used was Aluminum 2x38 mm.

The maximum flow in the same system without the valve installed was above 584,23 l/hr. This results in a flow reduction of more than 50% compared to when the valve was installed. The analytical model predicted that the maximum Reynold's number for this valve using an inlet-pressure of 6 bar would be 616.88. The flow is considered to be laminar.

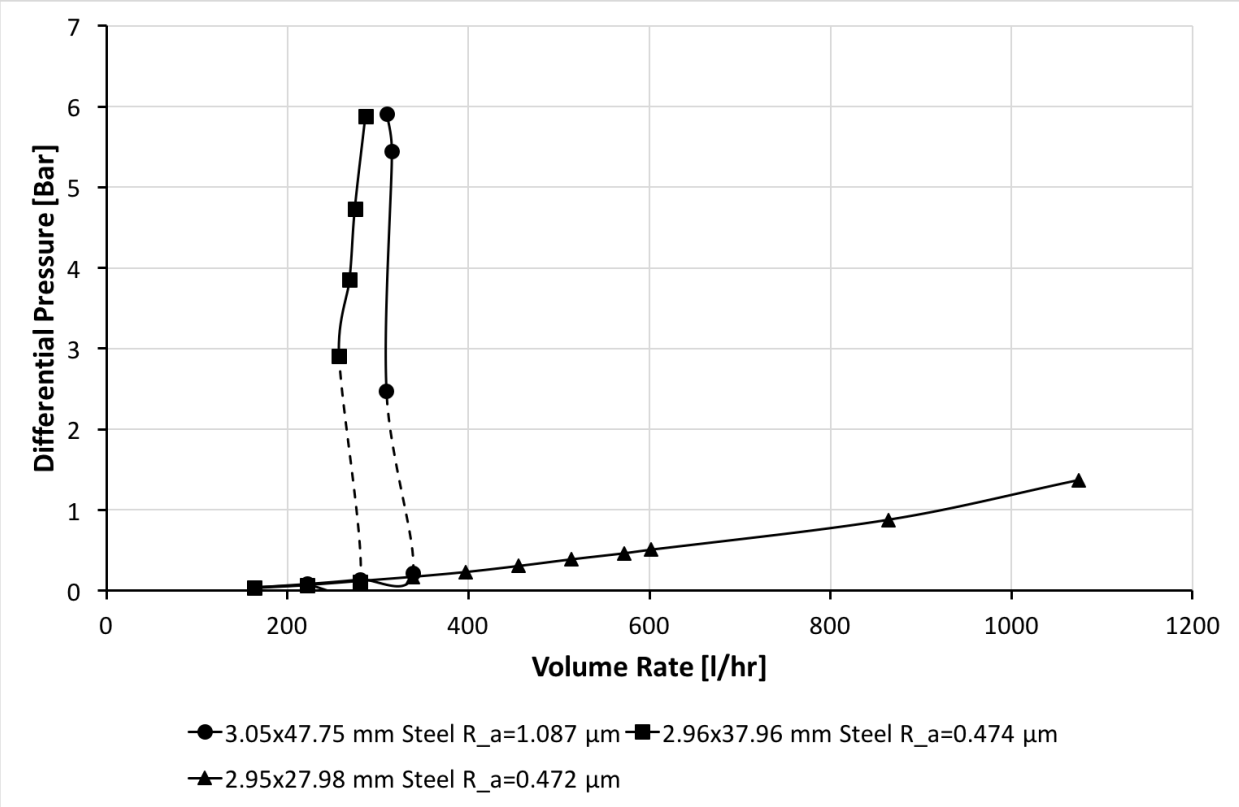

Figure 30: Performance results for 3 mm plate in valve sizes. As seen the 30 mm valve was unable to choke the flow exponentially

Figure 30 shows that the 30 mm valve was unable to choke the water flow. The 30 mm valve had a linear pressure vs. flow curve as opposed to the exponential increase seen in the 40 mm and 50 mm valve. Dotted lines in Figure 30 indicate the pressure surge when the plate started choking the flow.

5.1.2 Oscillations

Figure 31 shows the frequency spectrum for different flow rates and differential pressures across the valve. An energy increase in the frequency spectrum was observed at lower frequencies when the valve was choking the flow. A loud noise was observed at high differential pressure.

This indicates that the plate was oscillating when the valve had a large pressure-loss. This energy increase was not observed when the valve had a low pressure loss(before the exponential differential pressure increase). Figure 31a shows the frequency spectrum at 165.5 l/s with a negligible pressure loss across the valve. There are no dominant frequencies observed at 165.5 l/s, this indicates that the plate was pushed away from the valve-seat and in an open position.

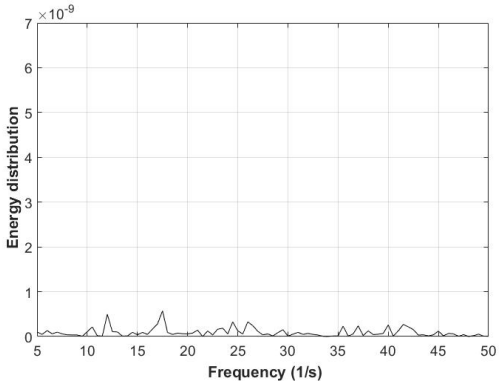

(a) Frequency spectrum of the valve when it was not yet choking at a flow of 163.5 l/s

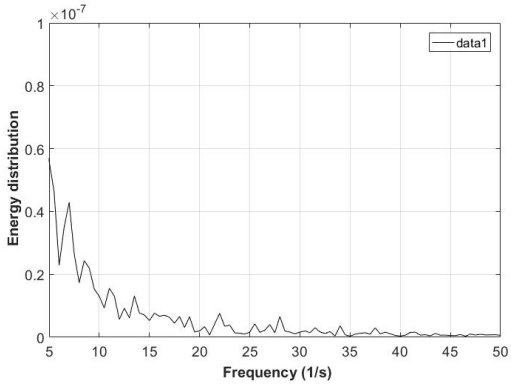

(b) Frequency spectrum of the valve when it was choking at a flow of 262.8 l/s

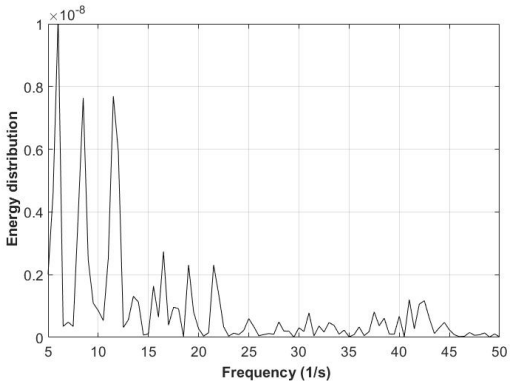

(c) Frequency spectrum of the valve when it was choking at a flow of 297.94 l/s

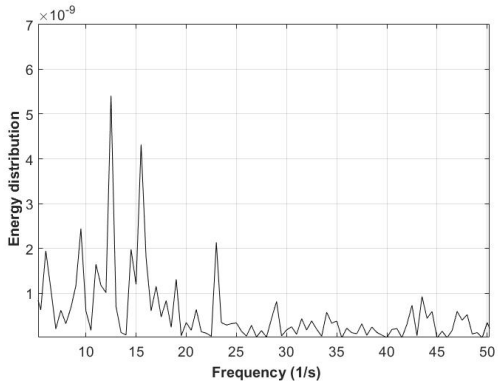

(d) Frequency spectrum of the valve when it was choking at a flow of 310 l/s

Figure 31: Frequency spectrum of 2mm plate in 40mm RCP valve

There was little consistency of the dominant frequency when the valve was choking the flow. In figure 31b there are no energy peaks, only a energy increase was observed at lower frequencies. Figure 31c and Figure 31d shows several different energy peaks at different frequencies. There seems to be some sort of dominant frequency around 5-20 Hz. It can be seen that the energy peaks in Figure 31c are similar to the energy peaks in Figure 31d. As the flow rate increases the energy in the frequency spectrum shifts to the right.

In this case a higher flow rate corresponds to a higher pressure. Therefore it seems as if the plate oscillates faster with a higher pressure-drop.

5.1.3 Plate Roughness and uniformity

There is no clear correlation between the surface roughness of the different plates and the choking effect. It is seen in Figure 32 that plate (a) with the lowest surface roughness has the best choking effect. However, plate (d) with the highest surface roughness has the second best choking effect. This indicates that there is no clear correlation between the choking effect and the surface roughness. The maximum Reynold's number predicted by the analytical model for the 50mm valve using a inlet-pressure of 6 bar was 500.4882. The flow is considered to be in the laminar regime.

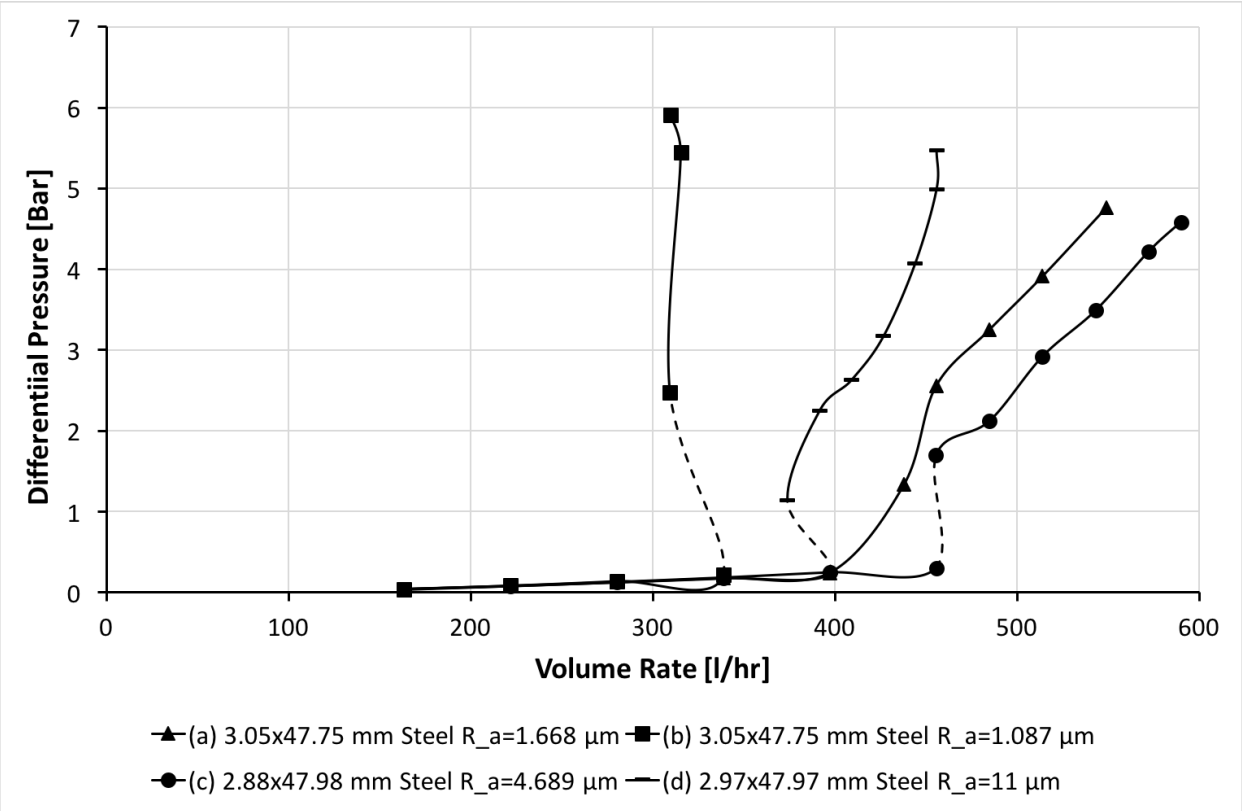

Figure 32: Performance results for 3x48 mm plates with different surface roughness

Dotted lines in Figure 32 indicate the pressure surge when the plate started choking the flow. It is dotted because it was not possible to obtain any results between the last point before choking and when it was choking.

There is a uniformity difference seen when comparing the plate (a) with the lowest surface roughness with the rest of the plates as seen in Figure 33. Plate (a) has a lot more uniform plane than the rest of the plates. The other three plates in Figure 33 shows a concave shape. This correlates nicely with the choking effect seen in Figure 32, this plate has a lot better choking effect than the other three plates.

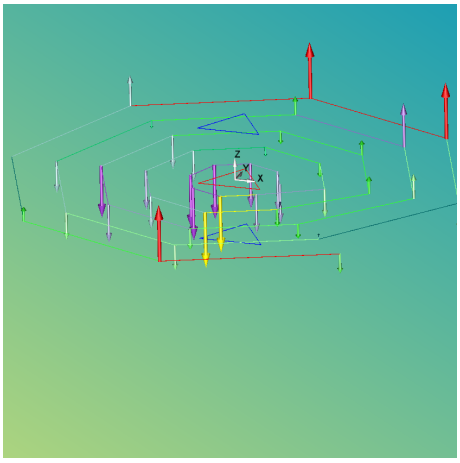

(a) Uniformity measurement of 0.01 mm and surface roughness $R_a = 1.087\ \mu m$

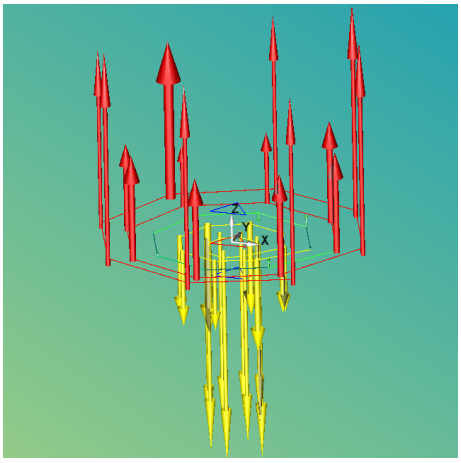

(b) Uniformity measurement of 0.066 mm and surface roughness $R_a = 1.668\ \mu m$

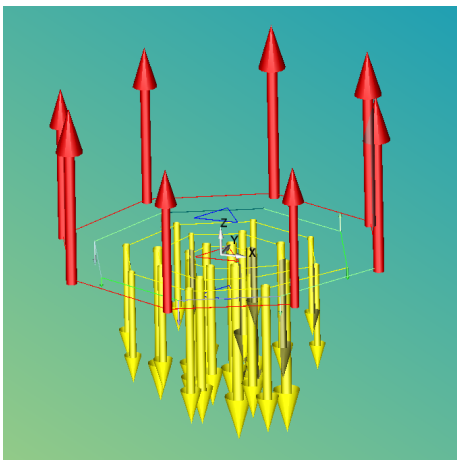

(c) Uniformity measurement of 0.045 mm and surface roughness $R_a = 4.533\ \mu m$

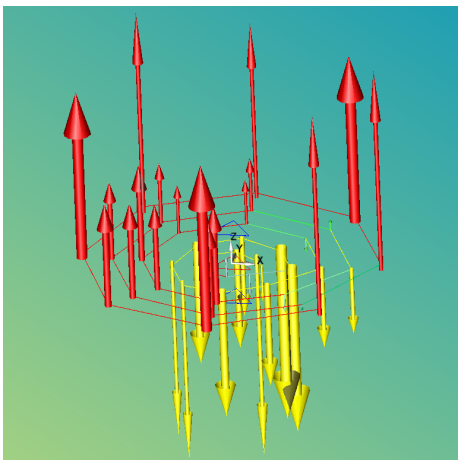

(d) Uniformity measurement of 0.059 mm and surface roughness $R_a = 11.00\ \mu m$

Figure 33: Uniformity measurement of 50mm steel plates. It shows that there was a large variation between the plane uniformity of the different plates.

It is more difficult to explain the difference in the choking effect between the three other plates (the ones with concave shape). It is seen from Figure 33c that even though it still has a concave shape, its outer edge is a lot smoother than what is seen in Figure 33d and Figure 33b. This might explain the reason why the plate seen in figure 33c has a better choking effect. However, it is important to note that even though the plate seen in Figure 33c looks like it had a more even concave shape, all the last three plates had a uniformity measurement that was similar. On the other hand, these results indicate that the uniformity of the plate plays an important role in deciding the choking effect of the valve. As the flow enters the valve it flows radially onto the plate and the choking effect occurs when the plate is drawn to the seat. When the plane of the plate is uneven compared to valve seat it may not choke optimally as the plate was not able to sit on the valve-seat. It is also important to compare the uniformity of the valve-seat as seen in Figure 23 to the plate uniformity. It is seen that the 50mm valve-seat had a convex shape, therefore, the plate with the concave shape might have a better choking effect than the plane/flat plates. It might be that even though a plate has a more uneven plane, it 'sits' better on the valve-seat.

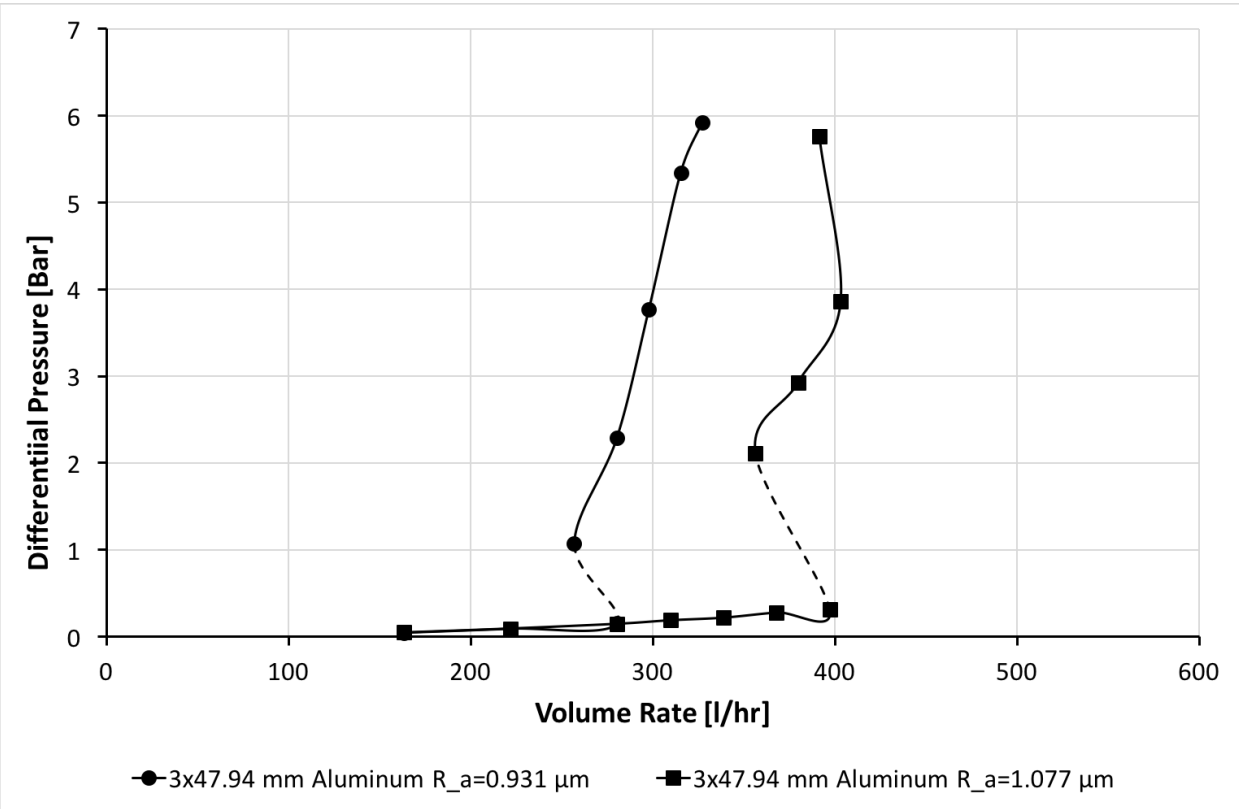

Figure 34: Performance of the 50 mm aluminum plate tested on both sides inside the RCP valve. There is a large variation between the two sides of the same aluminum plate.

Figure 34 shows the choking effect of both sides of the same aluminum plate in the 50mm valve. Both sides had a very similar surface roughness and exactly the same weight, thickness and radius. The best plate-side had a maximum flow rate of 327.04 l/hr with a pressure drop of 5.92 bar. The other plate-side had a maximum flow rate of 391.28 l/hr with a pressure drop of 5.76 bar, this is a difference in maximum flow rate of approximately 16%.

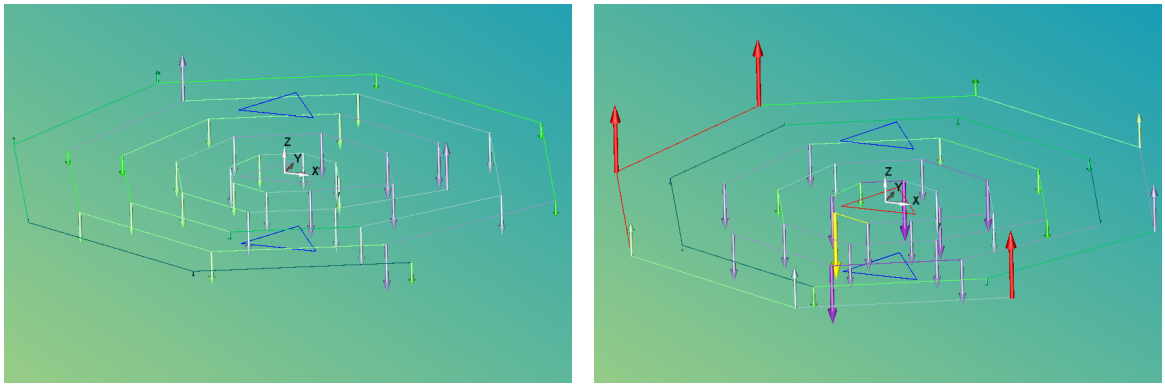

(a) 0.007 Surface uniformity of 3x47.94 mm aluminum plate with surface roughness $R_a = 0.931\ \mu m$

(b) 0.01 Surface uniformity of 3x47.94 mm aluminum plate with surface roughness $R_a = 1.077\ \mu m$

Figure 35: Plane uniformity measurement of the 50 mm aluminum plates. There is a small difference in plane uniformity between the two different sides of the same plate

The only difference between the two sides is a small difference in surface roughness and a difference in uniformity. Figure 35a had the best choking effect and also the best plane uniformity. The side of the plate seen in 35b has a lower plane uniformity. The difference in the choking effect indicates that uniformity of the plane and how the plate 'sits' on the valve-seat plays an important role in determining the choking effect. Although the plane uniformity is different for the two plates, it is not very large.

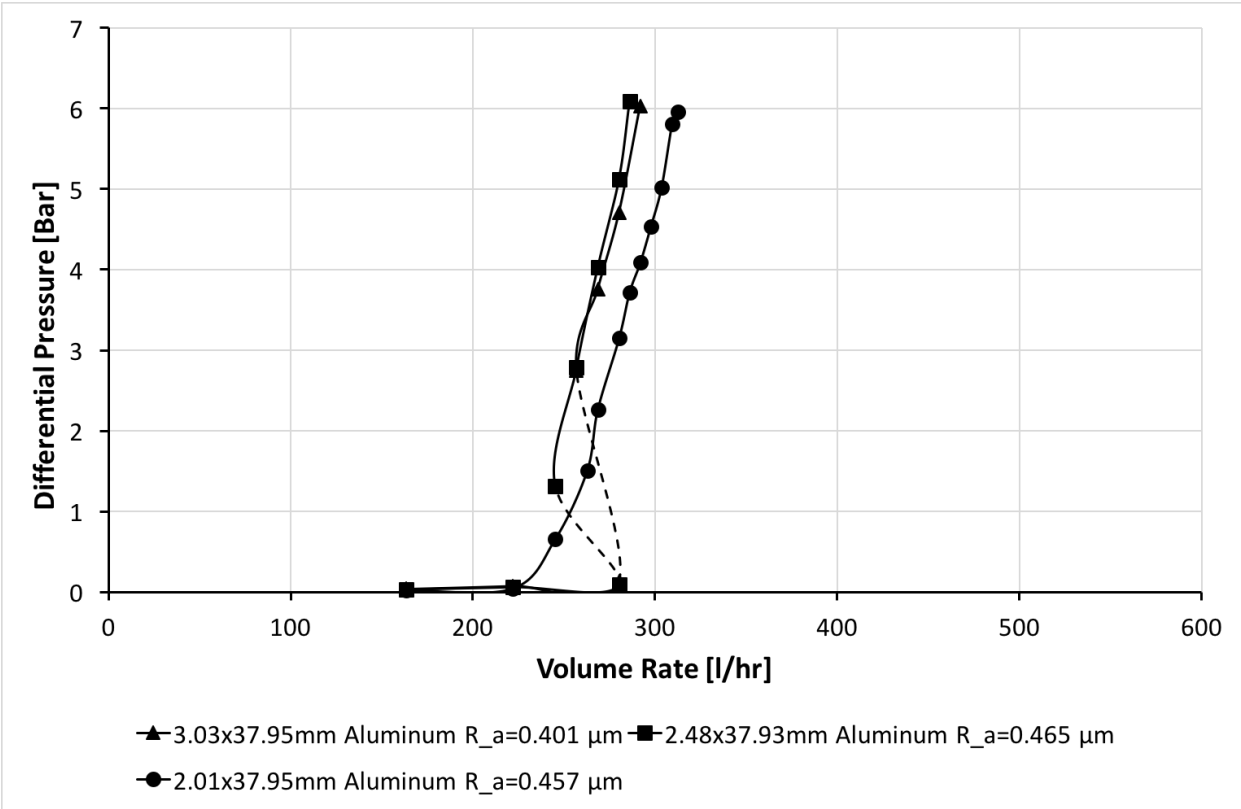

Figure 36: Performance results for the 40 mm valve with three different plate sizes in aluminum.

Figure 36 shows the pressure drop across the 40 mm valve using three different aluminum plates with varying thickness. Two of the plates with a thickness of 3.03 mm and 2.48 mm shows a very similar pressure vs. flow curve. Both of the plates had a maximum flow rate of approximately 280 l/hr at approximately 6 bar. There was a difference in the closing sequence between these two plates and the 2.01mm plate. The two plates with the highest reduction in flow experienced a pressure surge at approximately at 280 l/hr. After this pressure surge the flow rate was reduced and the differential pressure across the valve increased significantly. This pressure surge was not observed in the 2.01mm plate, this plate simply experienced an exponential differential pressure across the valve as the flow rate increased. It was the behaviour seen in the 2.01mm plate that was predicted by the model.

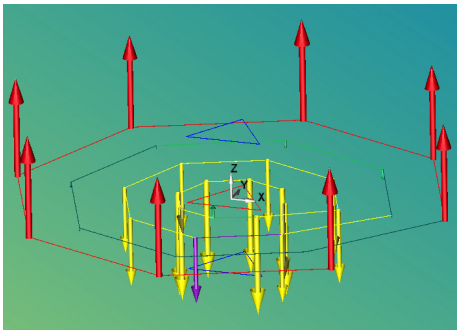

(a) 3.03 mm plate, uniformity parameter of 0.015 mm and surface roughness $R_a = 0.401\ \mu m$

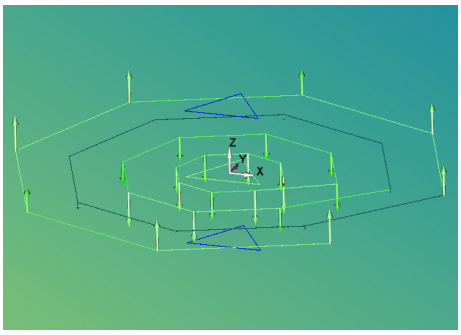

(b) 2.48 mm plate, uniformity parameter of 0.005 mm and surface roughness $R_a = 0.465\ \mu m$

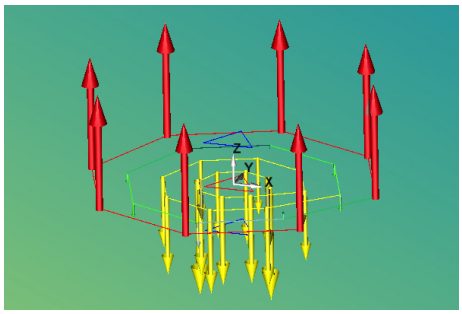

(c) 2.01 mm plate uniformity parameter of 0.026 mm and surface roughness $R_a = 0.457\ \mu m$

Figure 37: Uniformity analysis of 40mm Aluminum plates

The plate seen in Figure 37a had a concave shape with a plane uniformity of 0.015 mm whereas the plate in Figure 37b had a plane uniformity of 0.005 mm. It is therefore difficult to explain why the plates show a similar behaviour in the RCP valve. It was know from earlier the 40 mm valve had a plane uniformity of 0.004 mm. The plane uniformity difference of the plate in Figure 37a and the plate in 37b was low, this might indicate that the uniformity did not affect the choking effect. Figure 36 also indicates that there is a small difference in the choking effect due to the thickness of the plates. The thinnest plate had a lower reduction in flow compared to the two plates that were slightly thicker. However it may be that this difference in choking effect was due to the difference in plane uniformity as the plate in Figure 37c had the highest plane uniformity deviation.

5.2 Oil flow

5.2.1 Valve performance

All oil tests were done with Texaco Hydraulic Oil HDZ 32. This oil had a viscosity of approximately 64 centipoise at approximately 15 °C.

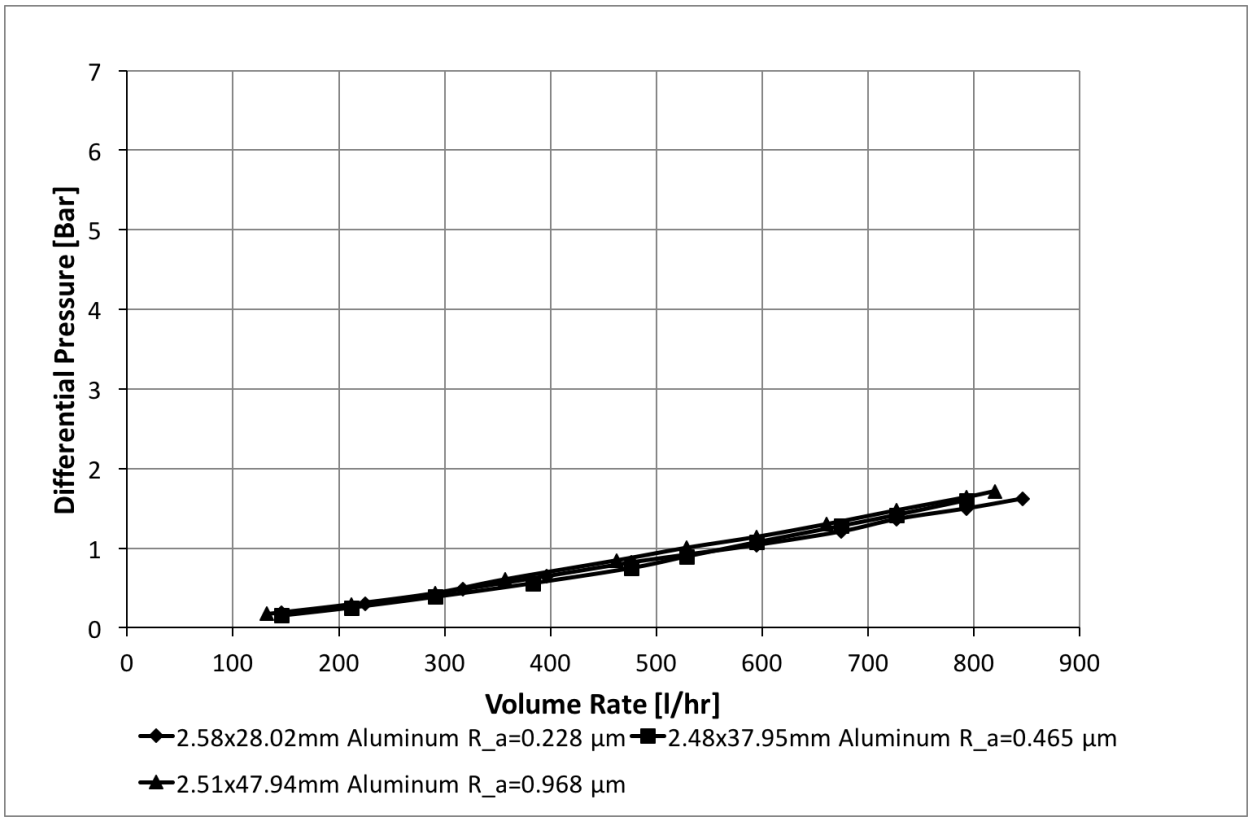

Figure 38: Performance results for 2.5 mm smooth aluminum plates for three valve sizes

As seen in Figure 38 the curves were almost linear. The performance curves indicated no Bernoulli choking effect. It was likely that the pressure increase seen in Figure 38 was due to a throttling effect. The radial size of the valve does not seem to affect the choking effect.

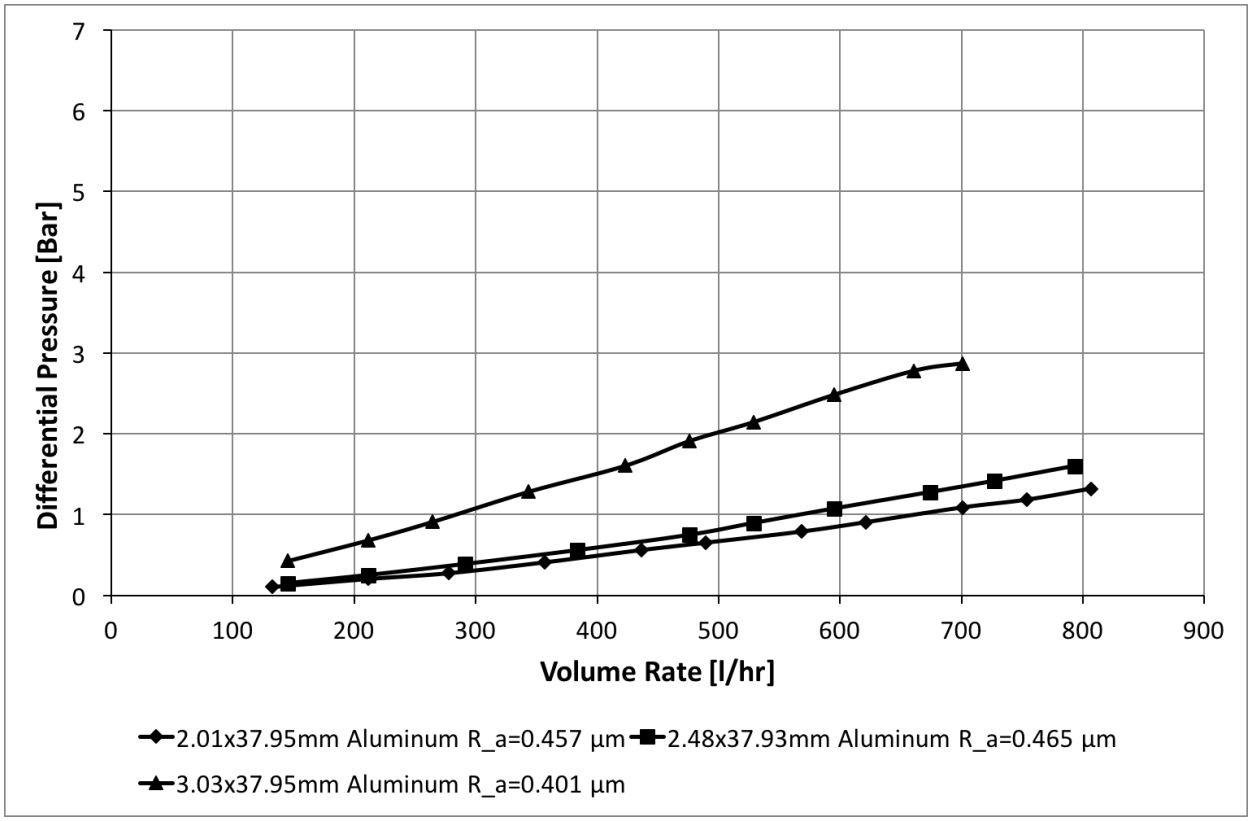

Figure 39: Performance results for the 40 mm valve with three different plate sizes in aluminum

As seen in Figure 39, the curves were linear and there was no exponential choking effect. The plates seen in figure 39 had slightly different performance even though all three plates had similar surface roughness. The 3.03 mm plate had the highest differential pressure and the 2.01 mm plate had the lowest differential pressure. The 2.01 mm plate and the 2.48 mm plate had similar performance with a small difference in differential pressure at higher flow rates. This indicates that pressure drop across the valve increased with higher plate thickness.

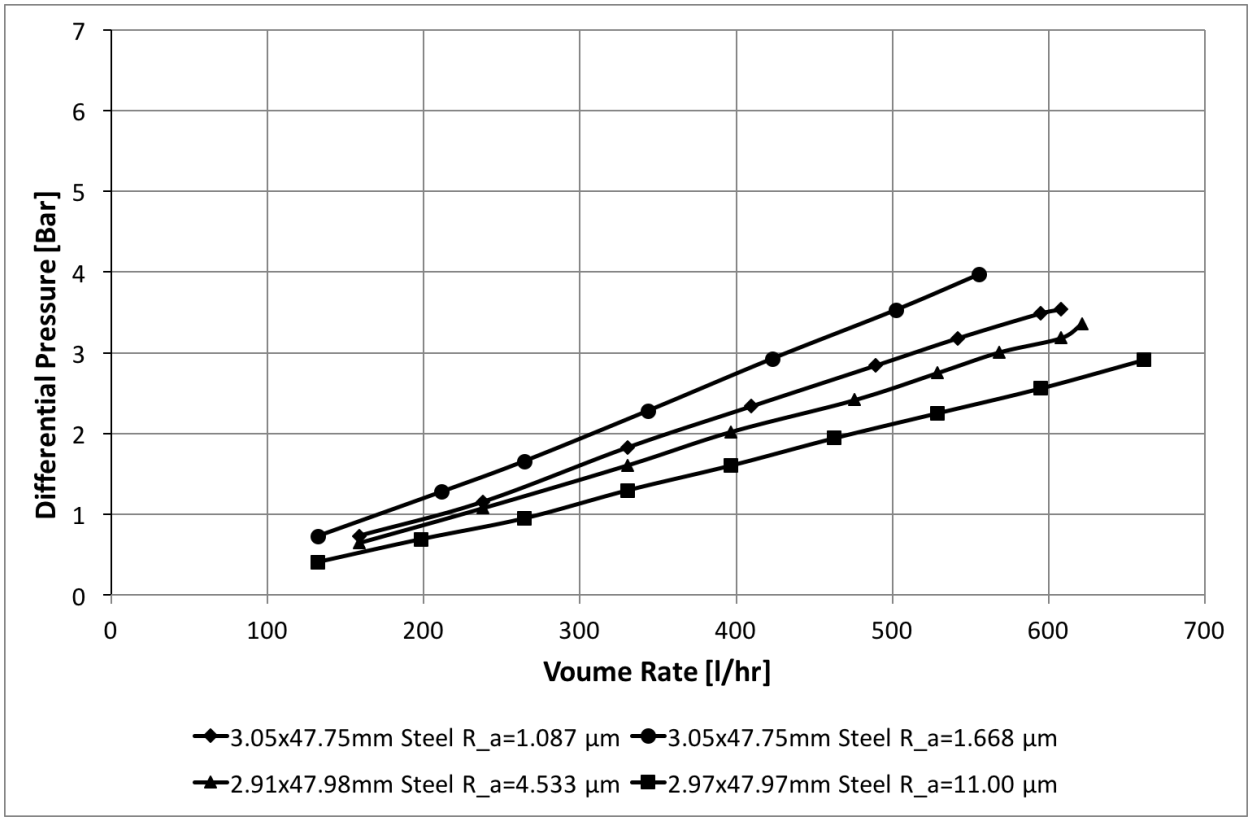

Figure 40: Performance results for 3x48 mm plates with different surface roughness

All plates in Figure 40 were approximately 3 mm thick. Therefore, the maximum column opening was approximately one millimeter. Even though the plates had approximately the same thickness there were large variations in the performance. The plate-side with the second lowest surface roughness had the highest differential pressure and was 3.05mm thick. The plate with the highest surface roughness had the lowest pressure drop across the valve, this plate was also 0.08mm thinner than the plate with the highest pressure drop. These plates had different thickness, uniformity and surface roughness.

5.2.2 Oscillations

There was no dominant frequency when testing the 40 mm RCP valve with the hydraulic oil. The analytical model predicted a low Bernoulli choking effect for the oil tested. In Figure 41 the frequency spectrum shows a flat distribution. This indicates that there were no oscillations and the plate was in an open position(pushed away from the valve-seat). There was also no sound observed during the testing of oil.

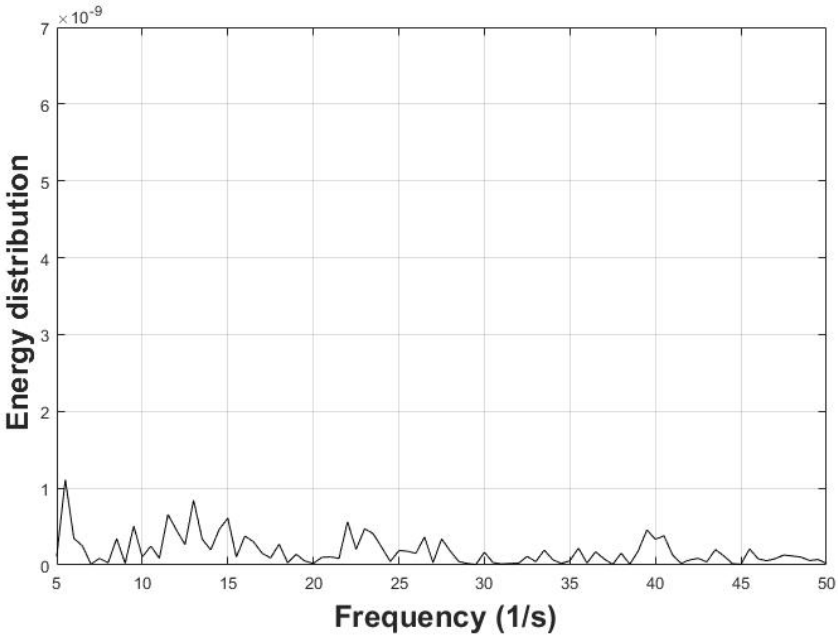

Figure 41: Frequency spectrum of oil in a 40mm valve with a 3 mm aluminum plate at 800 l/s

5.3 Gas Flow

5.3.1 Valve performance

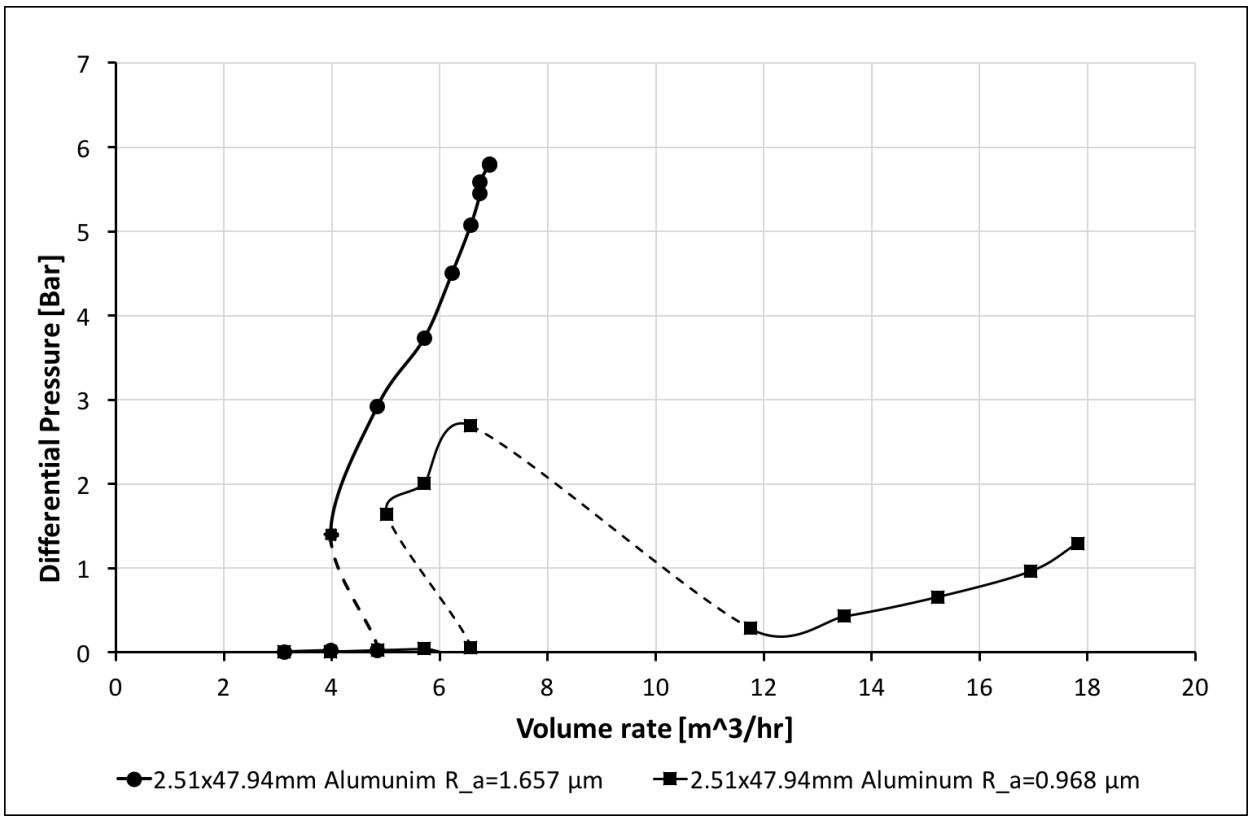

Figure 42: Performance results for a 3x48mm aluminum plate on both sides

The results in Figure 42 shows the the choking effect of a 2.51 mm plate in a valve with a valve-seat radius of 50 mm, both sides were tested due to different properties. The 2.51 mm plate with a surface roughness of $R_a = 1.657\mu m$ had a differential pressure of almost 6 bar at a flow rate of approximately 700 l/hr. At low rates this plate-side had a small gradual increase in pressure before the plate was drawn to the valve-seat and choked the flow. This resulted in a surge in pressure-drop across the valve.

The same pressure-drop surge was also observed with the 2.51 mm plate with a surface roughness of $R_a = 0.968\mu m$.

However, as the pressure built up there was an abrupt 'release' of the pressure at a volumetric rate of approximately 650 l/hr seen in the 2.51 mm plate. The plate was pushed away from the valve-seat and there was a reduced choking effect. If the flow was reduced back down, the valve started to choke again at lower rates.

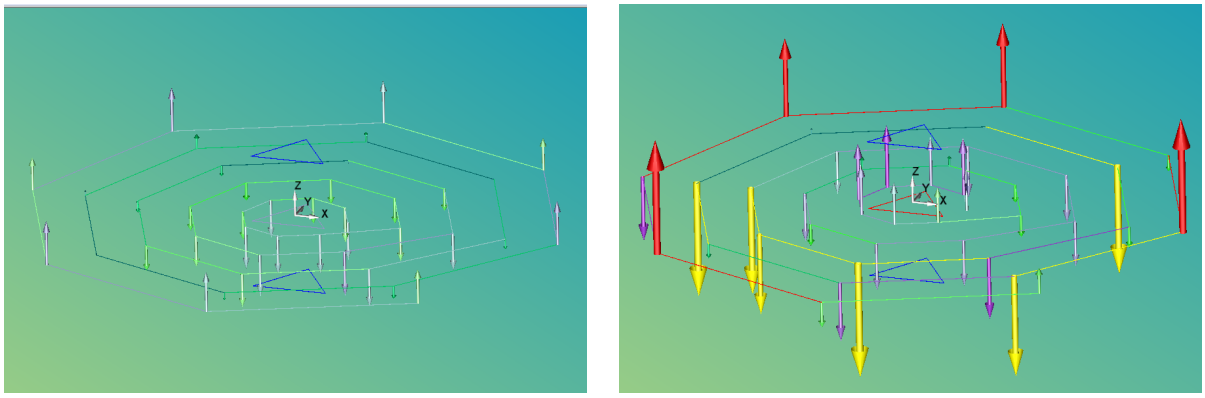

(a) Uniformity analysis 2,52x47,94 mm plate $R_a = 1,657\ \mu m$ aluminum with a uniformity of 0,007 mm

(b) Uniformity analysis 2,51x47,94 mm plate $R_a = 0,968\ \mu m$ aluminum with a uniformity of 0,017 mm

Figure 43: Uniformity measurement for the plates in Figure 42

Figure 43 shows is the uniformity measurement of the plates illustrated in Figure 42. As seen on Figure 43a the plate was almost perfectly flat, with a uniformity measurement of 0.007 mm. This flat surface correlates with the uniformity of the 40 mm valve. The surface seen on Figure 43b in more uneven with uniformity measurement of 0.017. The surface is also twisted with different heights throughout the surface. This may affect the choking capability of the surface. Compared uniformity with Figure 42 the results correlates nicely. The surface with best uniformity Figure 43a has a better performance curve.

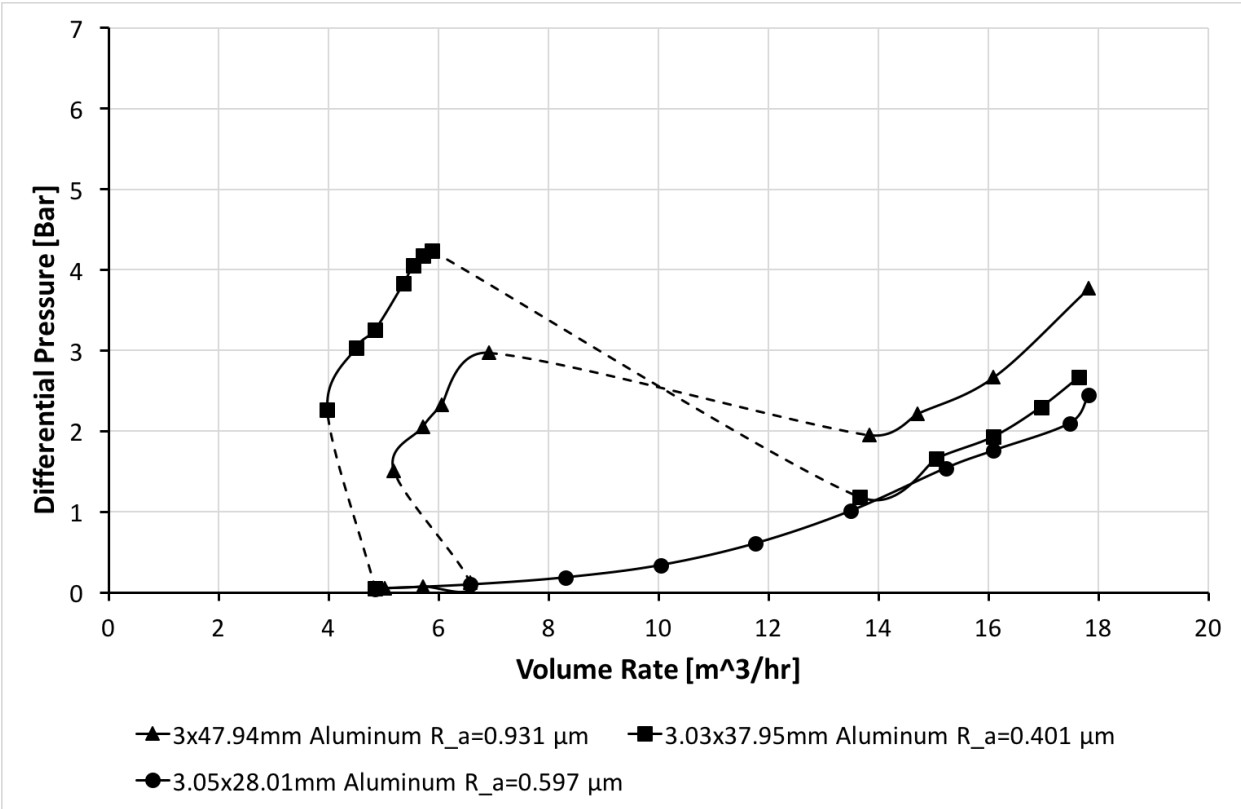

Figure 44: Performance results for the 3 mm aluminum plate in all valve sizes.

Figure 44 shows the test result of a 3 mm thick aluminum plate in three different valve-seat sizes. There was a large variation in the choking effect. The 30mm valve size exhibited a slow and gradual choking effect. The 40 mm valve had the best choking effect and the 50mm valve had the second best choking effect. At the same volume flow the 50 mm and 40mm valve had a large variation in the pressure loss across the valve. Both the 50 mm and 40 mm valve had an abrupt 'release' of pressure when the flow and pressure reached an upper limit for the valves. It was observed that the 40 mm had this 'release' at a higher flow rate than the 50 mm valve even though the 50 mm valve had a higher differential pressure.

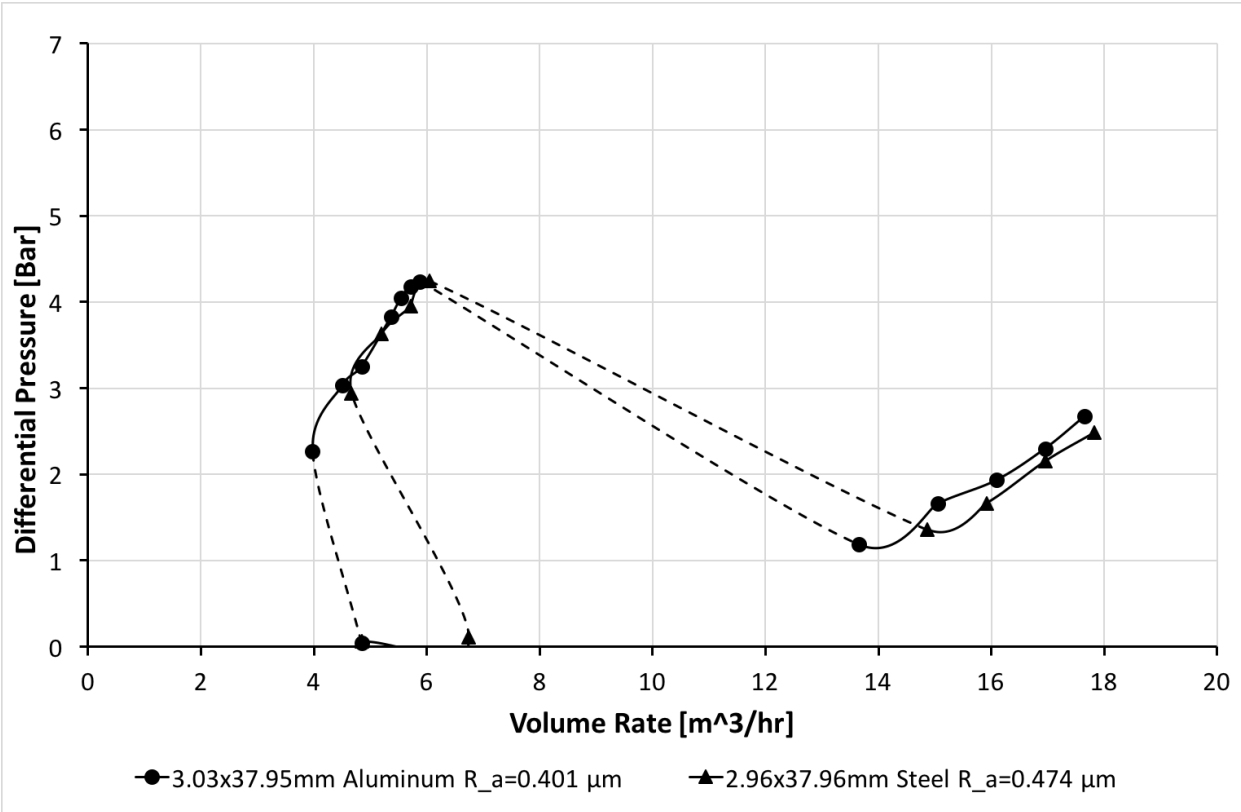

Figure 45: Performance results for 3x38 mm aluminum and steel plates.

Figure 45 shows the result when a stainless-steel plate and aluminum plate was tested with the same plate thickness. Both curves showed a very similar pressure vs. flow development. However, the aluminum plate chokes the flow earlier than the stainless-steel plate. Both plates 'release' the pressure approximately at the same conditions.

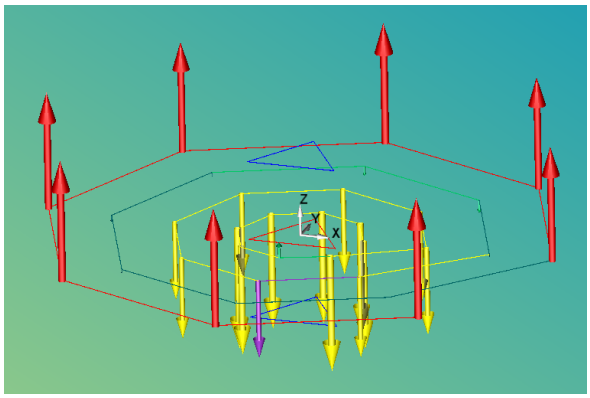

(a) Uniformity analysis 3,03x37,95 mm $R_a = 0,401\ \mu m$ aluminum with a uniformity of 0,015 mm.

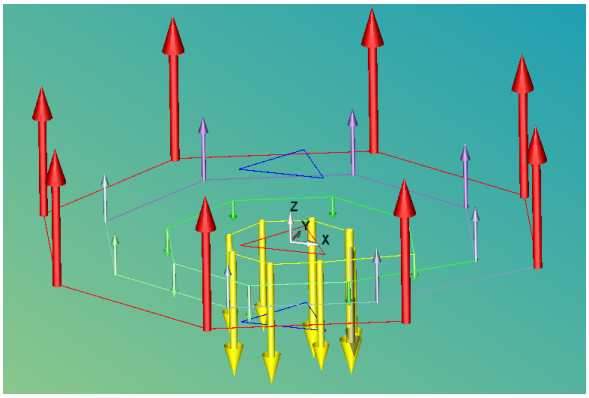

(b) Uniformity analysis of 2,96x37,96 mm $R_a = 0,474\ \mu m$ steel with a uniformity of 0,019 mm.

Figure 46: Uniformity results for the curves in Figure 45

As seen on Figure 46 the uniformity on the two surfaces are almost identical. The uniformity measurements were 0.015 and 0.019 and both surfaces were symmetrical. As they both were symmetrically uneven the uniformity measurement suggests they should perform equally. As seen on Figure 45 the testing results were overlapping. These results indicate that uniformity may affect choking.

5.3.2 Oscillations

Figure 47 shows the frequency spectrum when the valve was choking the gas flow and when it was not choking. There was a large difference between the energy peaks of the two spectres. Figure 47b at 6.2 m^3/hr and 4.5 bar shows a large energy peak at approximately 75 Hz and a smaller energy peak at approximately 140 Hz. The frequency spectrum in Figure 47a at 6.5 m^3/hr and approximately 0 bar is more evenly distributed with smaller peaks distributed along the x-axis. These small peak approximately at 50 Hz may be interpreted as the valve is attempting to draw the plate to the valve-seat. The high energy peaks seen in Figure 47b is most likely a result of the plate oscillating inside the valve. This was also supported by the very loud noise that was observed during testing.

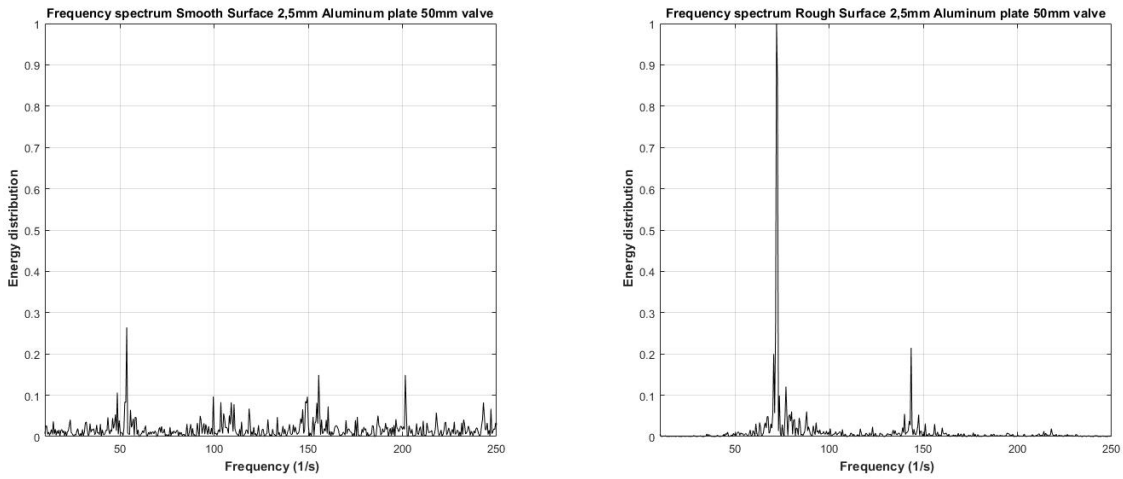

(a) Smooth plate at 6.5 m^3/hr and 0 bar. Evenly distributed energy.

(b) Rough plate at 6.2 m^3/hr and 4.5 bar. Energy peaks at 75 Hz and 140 Hz.

Figure 47: Frequency spectrum of 50mm valves with performance shown in Figure 42

6 Dicussion

6.1 Measurement and prediction

It was known a-priori that the RCP valve has a selective choking effect based on the fluid viscosity. Halvorsen et. al. showed in the paper from 2012 that gas and water had a much steeper differential pressure vs. flow curve than oil[1]. However, there was little background information as to how the valve choked the flow of low viscosity fluids. The analytical model presented in Chapter 3.3 was an attempt to better understand the working principles of the RCP valve. This analytical solution is new and has never been published before.

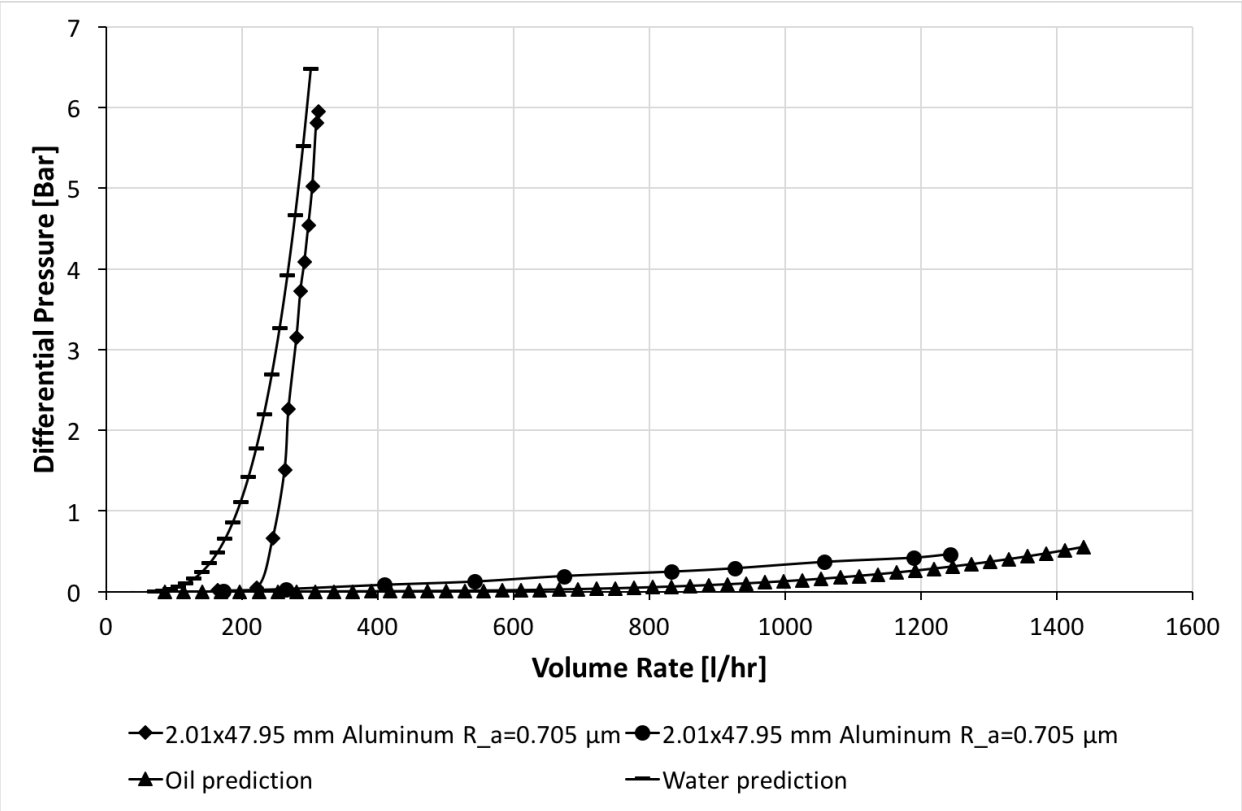

Figure 48: Performance results from oil and water testing with a 2x48 mm plate compared to the analytical prediction

In Figure 48 the performance of water and oil has been compared to the analytical model. The analytical model was modified to fit the 40 mm valve, viscosity and inlet-pressure of this experiment. The model was able to predict the pressure vs. flow development for both oil and water. The analytical model predicted an exponential curve for water, the experiments for water had an almost straight vertical curve.

The model predicted that the valve would gradually lift the plate and reduce the water flow accordingly. In the experiment it was observed that the valve would either lift the plate or not lift the plate at all, resulting in a choke or no choke condition.

When testing oil the differential pressure was small compared to water. The model data correlated nicely with the experimental data. The experimental data showed a linear increase in pressure loss as the flow rate advanced. The model showed a non-linear, but small increase in the performance.

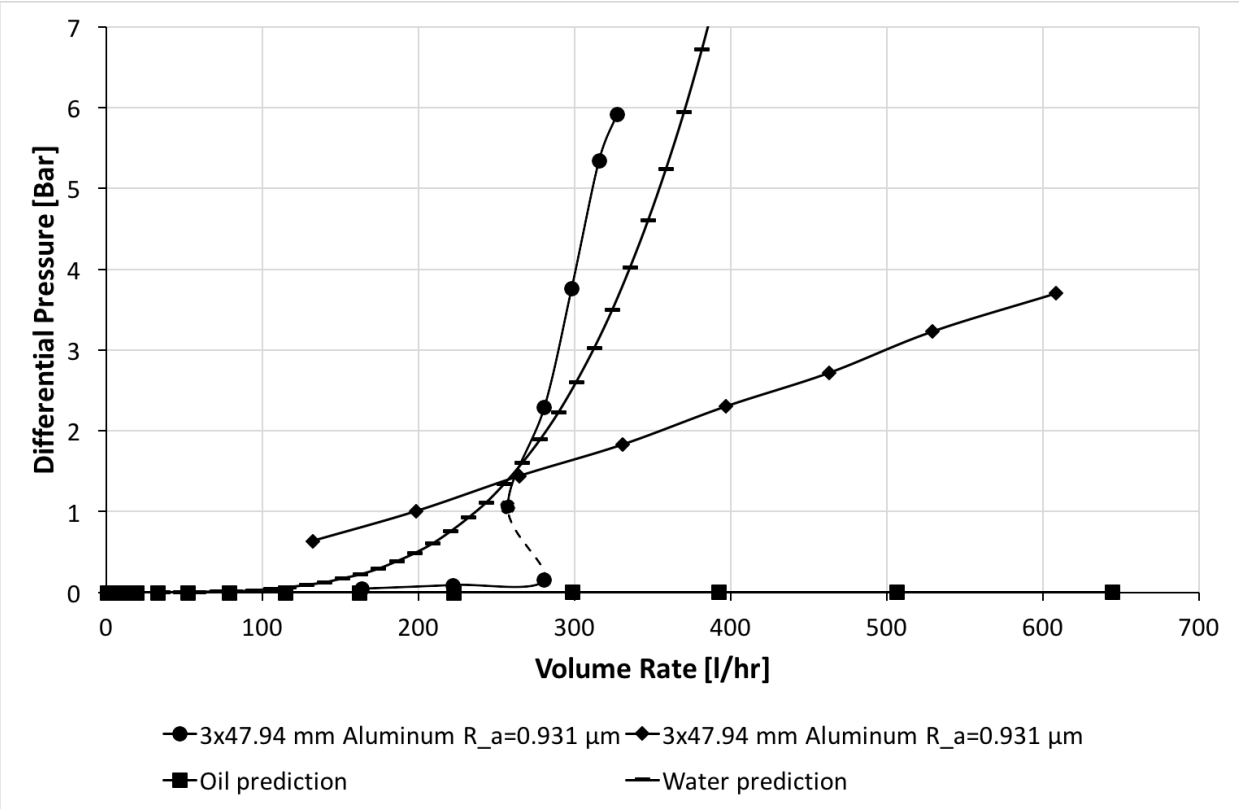

Figure 49: Performance results from oil and water testing with a 3x48 mm plate compared to the analytical method

Figure 49 shows the experimental results for water and oil in the 50 mm valve together with the model. The model was corrected for valve size, inlet-pressure and viscosity. As mentioned before the dotted line is not an observation, this was a surge in pressure loss across the valve. In this case, the experimental water exhibited a better choking effect than the model.

The oil results seen in Figure 49 had a pressure loss that was greater than what was seen in Figure 48. This was likely due to the clearance in the column opening between the valve-seat and the plate. This experiment was done using a 3 mm plate which lead to a small column opening of roughly 1 mm. The analytical model does not take into account the column opening between the valve-seat and the plate.

There was a large difference in the pressure vs. flow curves for oil and water. As predicted by the analytical model the choking effect was dependent on viscosity and density of the different fluids. The density of the oil tested was 857 kg/m^3 and the density of water was assumed to be 1000 kg/m^3. The choking effect seems to be more dependent on the viscosity rather than the density. The analytical model suggested that the choking effect is inversely proportional to the viscosity squared. The difference in viscosity was a lot higher than the density. The oil had a viscosity of 64 cp, the water had a viscosity of 1 cp. It is therefore difficult to conclude how much the choking is dependent on the viscosity when testing. A limitation to this experiment is that only one high viscosity oil was tested. To make a better conclusion oils of different density and viscosity should have been tested.

6.2 Plate thickness & column opening

As was seen in Figure 17 the analytical model predicted a small column opening when the valve was choking water. The opening ranged from 0.7 mm to almost 0 mm. This suggested that plate thickness was insignificant, as long as there was a column opening that was at least 0.7 mm. This was supported by the result when the 40 mm valve was tested with water using three different plates of varying thickness 2 mm, 2.5 mm and 3 mm. This result was seen in Figure 36 and shows that the choking effect of the three different plates was very similar. The main difference between the three plates was the development of the pressure vs. flow curve. Likely, this was due to variation in the plate plane uniformity and the surface roughness. However, due to the limitations of the testing facilities it was not possible to verify this. Other tests confirmed that the density of the plate did not affect the choking ability of the valve. Having said this, there were no other parameters that were different inside the valve other than the surface roughness and the plate plane uniformity. This leads to the conclusion that either plane uniformity or surface roughness affected the choking effect, possibly both.

In Figure 39 a large variation in the performance for different plate thicknesses was observed. It was clear when testing oil that column opening affected differential pressure. When testing water the column opening did not seem to affect the performance.

6.3 Plate uniformity and surface roughness

It was not exactly clear how the surface roughness and plate plane uniformity affected the choking effect. There were some trends that indicated that plates with worse plane uniformity had a reduced choking effect. But other results showed the opposite. It might be that even though a plate had worse plane uniformity, the plate itself had a better 'fit' with the valve-seat as this was not plane either. This would result in a more evenly distributed radial flow from the inlet across the plate. If the valve was not plane, the flow may have been skewed to one side of the plate. A limitation to this experiment was that all plates had a relatively similar plane uniformity. It would have been better to create plates that were uneven on purpose in order to test this theory. Therefore, it was difficult to make any conclusion as to how the plane uniformity affected the choking effect. The equipment used to make the valve and plates in this experiment was not accurate enough to determine the relationship between the uniformity and the choking effect. If more advanced manufacturing equipment had been used a final answer to this could have been obtained.

The surface roughness might also have affected the choking effect of the valve. In some cases such as when testing water in the 50 mm valve with different steel plates, there was a large variation in the choking effect of the valve. However, this reduced choking effect was difficult to correlate with the surface roughness of the plates. One explanation proposed was that the development of the radial flow inside the RCP valve is dependent on the surface roughness. It turns out that the transition from laminar to turbulent flow also depends on the degree of disturbance of the flow by surface roughness, pipe vibrations, and fluctuations in the flow[7]. Having said this, it is clear that the valve exhibits all of these conditions with surface roughness varying for all the plates used. Therefore, the variation of the choking effect might be results of how the flow develops inside the valve. A fluid flow will either be laminar, transient or turbulent. In the analytical model laminar flow was assumed. If the flow was assumed to be turbulent or transient the model would be a lot more complicated.

For some of the data sets the model accurately predicts the experimental pressure vs. flow curves. This might indicate that the curves that were accurately predicted show a more laminar flow than the plates that did not correlate with the model. One way to estimate the flow-regime is by calculating the Reynold's number. The model predicted a Reynolds number between 500-600 for both the 40mm and 50mm valve when testing water. This means that the flow is most likely laminar as this is below 2300 (this is originally the limit for flow in pipes, however it is assumed to be valid for this valve as the Reynold's number is relatively low). Therefore, a possible explanation to the variations in the choking effect with the different plates might be the differences in the flow regime.

6.4 Oscillation

The results showed that there was a relationship between the frequency spectrum and the choking of the valve. As stated in the background for the experiment, it was not easy to predict whether the plate would have a stable position inside the valve or if the plate would oscillate. Oscillations in the inlet-pressure was observed when the valve was choking water and gas flow. For each measurement during choking there was a slightly different frequency spectrum. When the valve was not choking the flow there were no energy peaks in the frequency spectrum. There was also no oscillations observed when the valve was flowing oil. This indicates that the plate was pushed away from the valve-seat and the valve was in an open position. This was also supported by the observed noise during testing of gas and water. This noise indicated that the plate was oscillating inside the valve. The loudest noise was observed when testing gas. The gas frequency spectrum also shows the most dominant frequencies. It was observed that gas had higher frequency vibrations than water. The reason for this might simply be that the gas was flowing faster than the water because the gas viscosity was lower. Oscillations like this may be harmful during the lifetime of a field. The oscillations might cause vibration and even resonance in the production tubing which might lead to decreased functionality of the well completion. All the individual vibrations caused by each valve might be a concern for the completion engineers.

For gas flow, compressibility and the pressure range made it impossible to compare the results to a reservoir. The gas experiment had a pressure ratio of six between inlet and outlet. In a reservoir this ratio would maximum be two and the gas would have higher pressure. Inside the valve gas will change characteristics and experience different velocities depending on the pressure. The velocity may exceed critical velocity in the low pressure area of the valve. The critical velocity effects might explain the abrupt release of pressure seen in the results when testing gas.

As the pressure changes through the valve the density of the gas will change. In the analytic solution it is seen that the choking effect is dependent on the density of the fluid. Although the analytic solution assumes an incompressible fluid this might indicate that the compressibility might influence the choking effect and therefore also the oscillations in the valve.

6.5 Recommendations for further work

Statoil's test illustrated a higher required flow for oil than water and gas in order to reach the choking pressure. In this experiment it was not possible to reach a sufficient oil rate to choke. The experiment was also limited because only one type of oil was tested, to make a better conclusion several oils with varying viscosity should have been tested. If several different oils were tested a trend for viscosity and choking could possibly been established. More testing with gas is recommended to better understand what happens when the plate starts to choke, but is not able to sustain the choke. It is also recommended to test the gas using pressures that are representative of oil fields. It was difficult to relate the gas testing results to real reservoirs because of scaling due to compressibility.

It would also be advantageous to manufacture the plates and valves using higher precision equipment. The plates could also be made uneven on purpose in order to test how the plane uniformity and surface roughness affects the choking effect.

A different setup when testing oil is also recommended in order to avoid emulsion between water and oil during testing.

7 Conclusion

The analysis and experiments show that the RCP valve has selective choking effect, in paticular letting viscous oil easier through than low viscosity water. For oil and water the model considered predicted valve performace corresponding to measurements.

For gas flow, compressibility effects is considerable and the analytical solution was no longer valid. Gas flow through the valve often caused oscillations, which may contribute to the characteristics measured.

When testing with oil the available column height between the valve-seat and the plate often limited the flow rate. This becomes an important design consideration to fully utilize the selective potential.

The surface roughness and plane uniformity affects the choking effect. It was observed that in general the plates with a smoother and more uniform surface had a better choking effect. However, with the experimental data available it was not possible to arrive at a firm and specific conclusion.

The ability to predict valve performance enables goal oriented design of rate controlled valves. Thus, the results obtained with the limits and uncertainties have obvious applications for production wells susceptible to water breakthrough. However, the unique characteristics of the RCP valve may have much wider application.

References

[1] Halvorsen, M., Madsen, M., Vikøren Mo, M., Isma Mohd, I., & Green, A. (2016, April 20). Enhanced Oil Recovery On Troll Field By Implementing Autonomous Inflow Control Device. Society of Petroleum Engineers. doi:10.2118/180037-MS

[2] Mathiesen, V., Werswick, B., Aakre, H., & Elseth, G. (2011, January 1). Autonomous Valve, A Game Changer Of Inflow Control In Horizontal Wells. Society of Petroleum Engineers. doi:10.2118/145737-MS

[3] Henriksen, K. H., Gule, E. I., & Augustine, J. R. (2006, January 1). Case Study: The Application of Inflow Control Devices in the Troll Field. Society of Petroleum Engineers. doi:10.2118/100308-MS

[4] Halvorsen, M., Elseth, G., & Naevdal, O. M. (2012, January 1). Increased oil production at Troll by autonomous inflow control with RCP valves. Society of Petroleum Engineers. doi:10.2118/159634-MS

[5] "The Troll Area." The Troll Area. Statoil, n.d. Web. 17 Nov. 2016. <http://www.statoil.com/en/OurOperations/ExplorationProd/ncs/troll/Pages/default.aspx>.

[6] Moses, Jonathon W. Transforming Resource Wealth into National Wealth: The Norwegian Model. Trondheim: NTNU, 2015. Print.

[7] Hibbeler, Russell Charles., and Kai Beng. Yap. Fluid Mechanics in SI Units. Harlow: Pearson Education, 2017. Print.

[8] Materiallære VG1. N.p.: Industri Skolen, n.d. Print. Accessed Online 5/25/2017

[9] Variable Area Flowmeters for Liquids and Gases. 9/86 ed. Vol. 1.1e. Horsham, PA: Fischer & Porter GmBH: Complete Process Instrumentation, n.d. Print. Repl. 7/83.

[10] Torsæter, Ole, and Manoochehr Abtahi. EXPERIMENTAL RESERVOIR ENGINEERING LABORATORY WORK BOOK. Trondheim: Department of Petroleum Engineering and Applied Geophysics, 2000. Print.

[11] Prof. Harald Arne Asheim at department of geoscience and petroleum ,harald.arne.asheim@ntnu.no, 73594959, personal interview

A Appendix

A.1 Plate measurement results

Table 1: Results of the 50 mm valve measurements

Type	Thickness [mm]	Diameter [mm]	R_a [μm]	R_z [μm]	Weight [g]	Spec	Uniformity [mm]
Steel	2.97	47.97	11.	44.5	40	Ultra rough	0.059
Steel	2.87	47.98	4.689	19	40	Medium rough	0.045
Steel	3.05	47.75	1.668	9.58	44	Rough	0.066
Steel	3.05	47.75	1.087	6.33	44	Smooth	0.01
Steel	2.47	47.64	0.639	4.18	34	Rough	n/a
Steel	2.47	47.64	0.302	2.37	34	Smooth	n/a
Steel	2.	47.86	1.815	9.01	28	Rough	n/a
Steel	2.	47.86	1.606	7.21	28	Smooth	n/a
Aluminum	3.	47.94	0.931	4.71	14	Smooth	0.007
Aluminum	3.	47.94	1.077	6.66	14	Rough	0.01
Aluminum	2.51	47.94	0.968	3.84	12	Smooth	n/a
Aluminum	2.51	47.94	1.657	7.72	12	Rough	n/a
Aluminum	2.01	47.95	1.409	6.72	10	Rough	n/a
Aluminum	2.01	47.95	0.705	4.52	10	Smooth	n/a

Table 2: Results of the 40 mm valve measurements

Type	Thickness [mm]	Diameter [mm]	R_a [μm]	R_z [μm]	Weight [g]	Spec	Uniformity [mm]
Steel	2.96	37.96	0.796	5.16	26	Rough	n/a
Steel	2.96	37.96	0.474	3.89	26	Smooth	n/a
Steel	2.51	37.95	6.99	30.06	22	Rough	n/a
Steel	2.51	37.95	2.398	10.4	22	Smooth	n/a
Steel	2.02	38.00	1.457	8.63	18	Rough	n/a
Steel	2.02	38.00	0.699	4.78	18	Smooth	n/a
Aluminum	3.03	37.95	0.401	2.64	8	Smooth	0.015
Aluminum	3.03	37.95	0.798	5.7	8	Rough	n/a
Aluminum	2.48	37.93	0.465	3.79	7	Smooth	0.005
Aluminum	2.48	37.93	1.02	6.13	7	Rough	n/a
Aluminum	2.01	37.95	0.644	4.5	6	Rough	0.021
Aluminum	2.01	37.95	0.457	3.15	6	Smooth	0.026

Table 3: Results of the 30 mm valve measurements (Rz)

Type	Thickness [mm]	Diameter [mm]	R_a [μm]	R_z [μm]	Weight [g]	Spec	Uniformity [mm]
Steel	2.95	27.98	0.472	3.72	14	Smooth	n/a
Steel	2.95	27.98	0.824	4.98	14	rough	n/a
Steel	2.54	27.96	0.204	1.74	12	Smooth	n/a
Steel	2.54	27.96	2.296	10.8	12	rough	n/a
Aluminum	3.05	28.01	0.597	2.74	5	Smooth	n/a
Aluminum	3.05	28.01	1.622	8.66	5	Rough	n/a
Aluminum	2.58	28.02	0.228	2.75	4	Smooth	n/a
Aluminum	2.58	28.02	1.111	5.87	4	Rough	n/a
Aluminum	2.1	28.01	0.288	2.29	3	Smooth	n/a
Aluminum	2.1	28.01	1.278	6.4	3	Rough	n/a

A.2 The original Bernoulli valve design

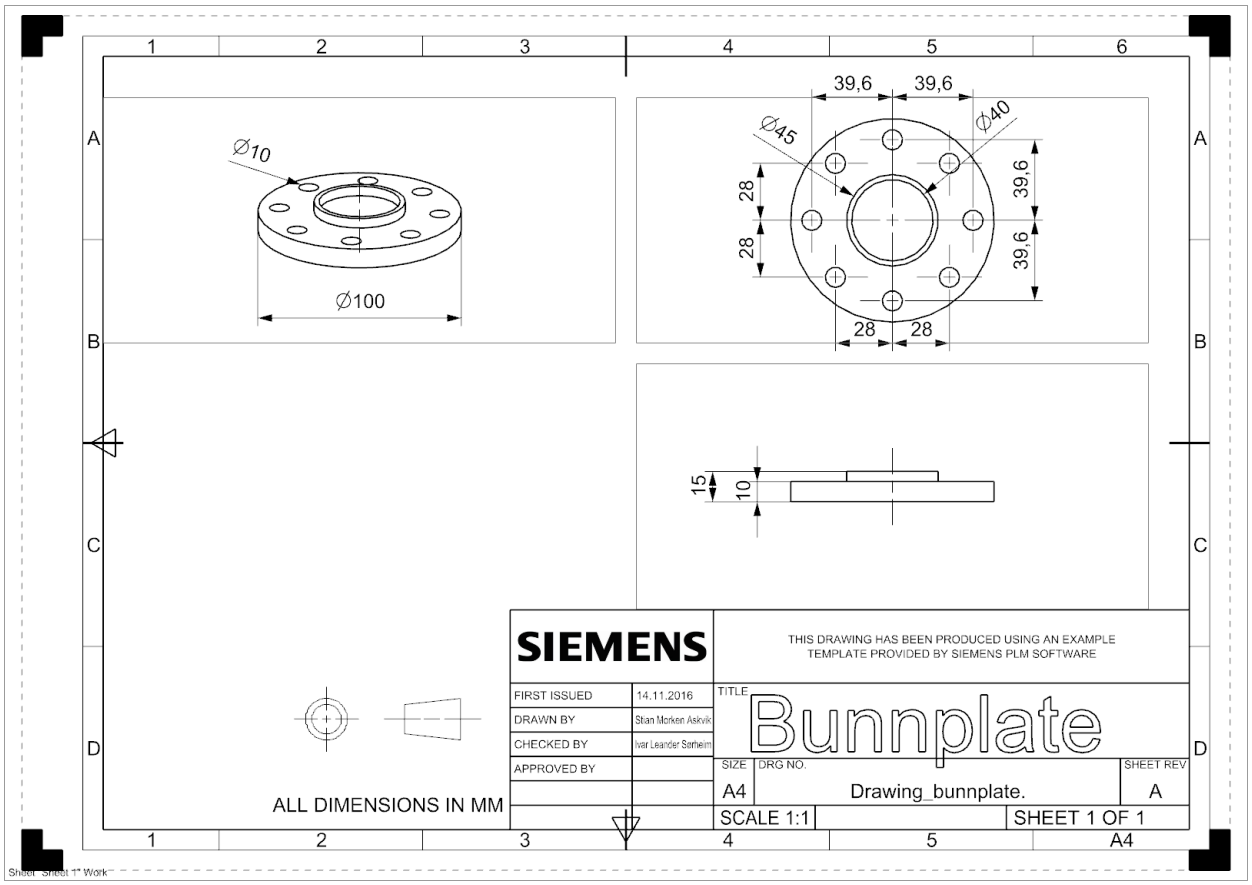

Figure 50: Drawing of bottom plate

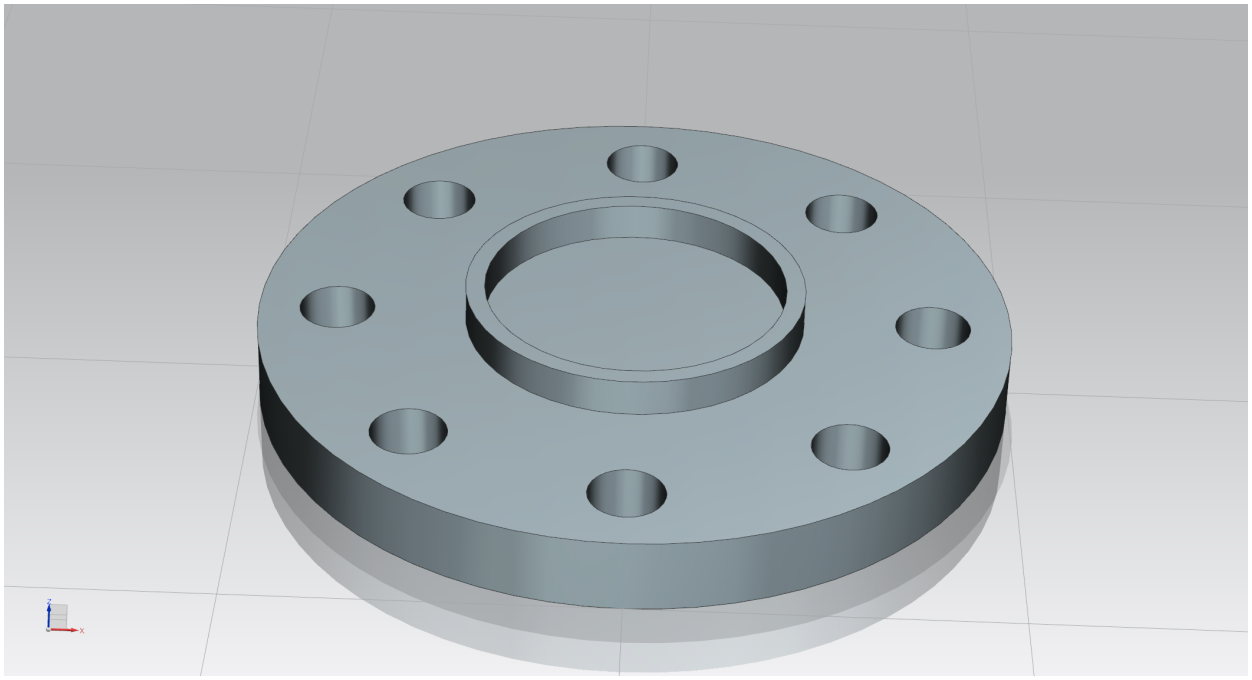

Figure 51: 3D illustration of the bottom part

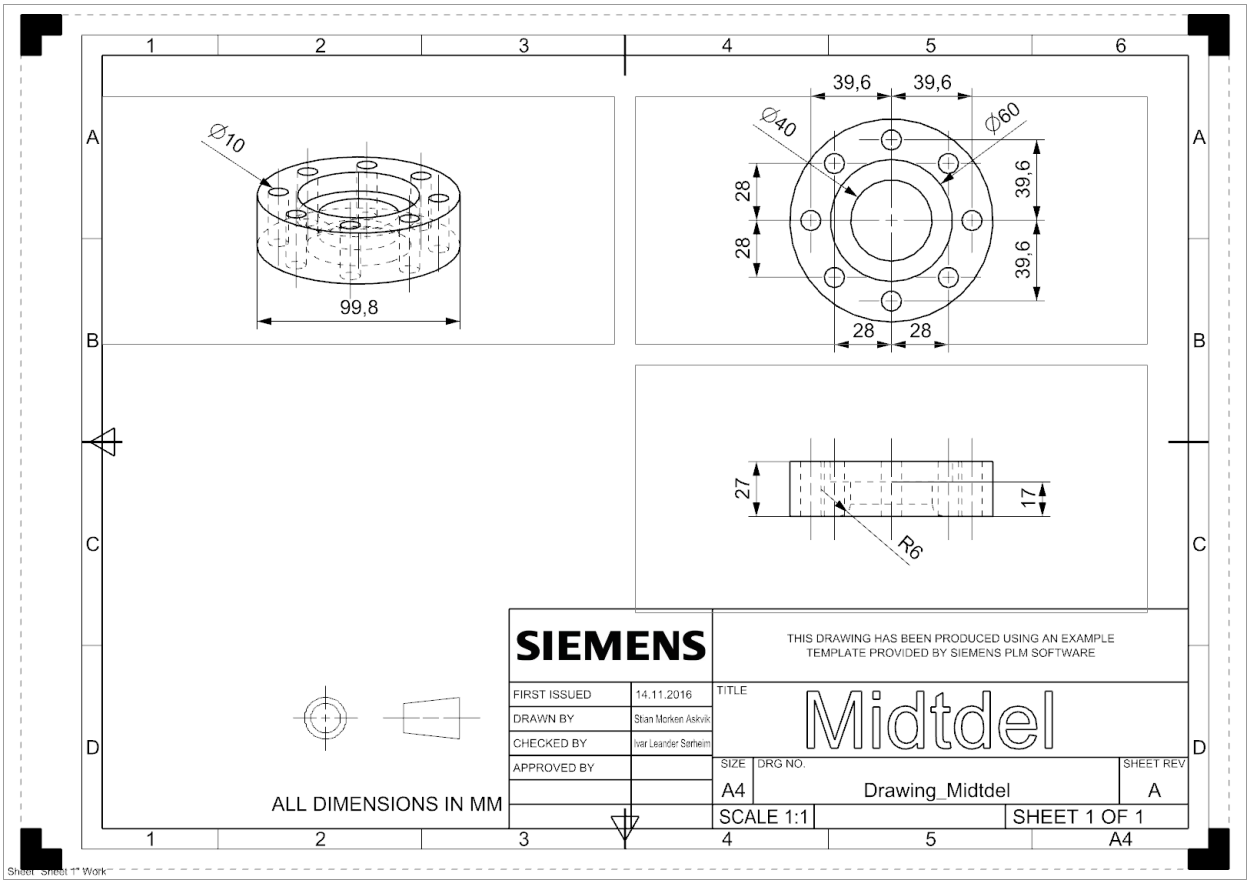

Figure 52: Drawing of the middle part

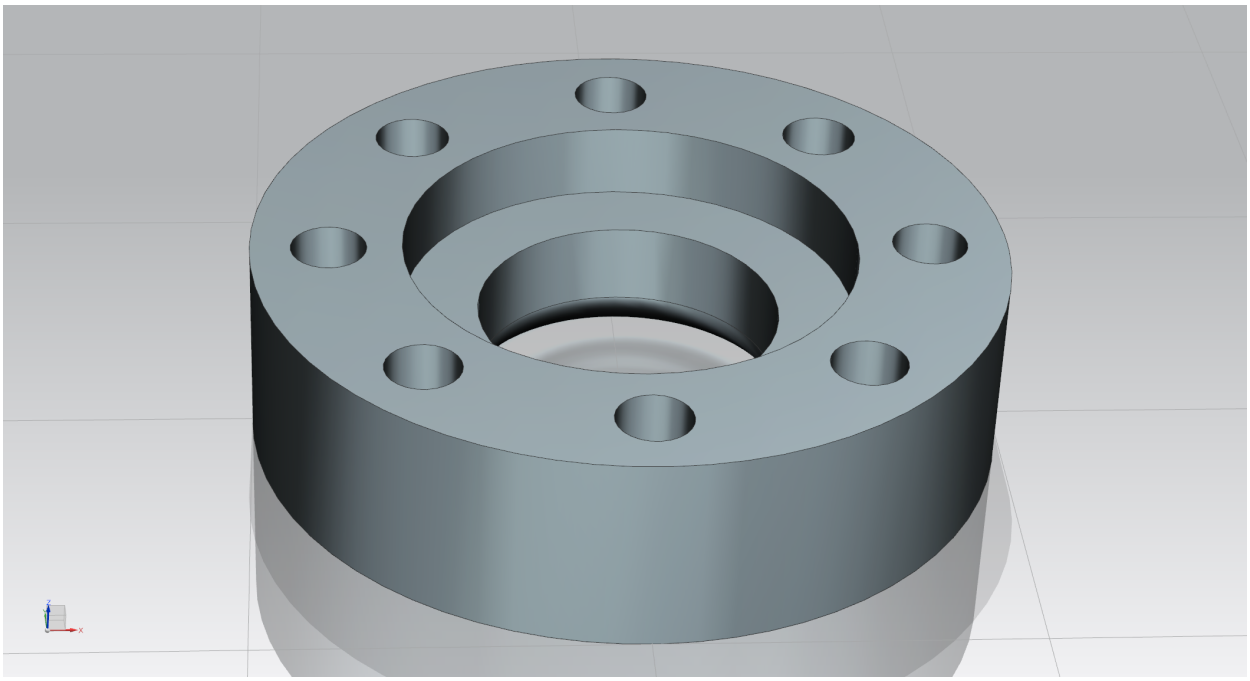

Figure 53: 3D illustration of the middle part

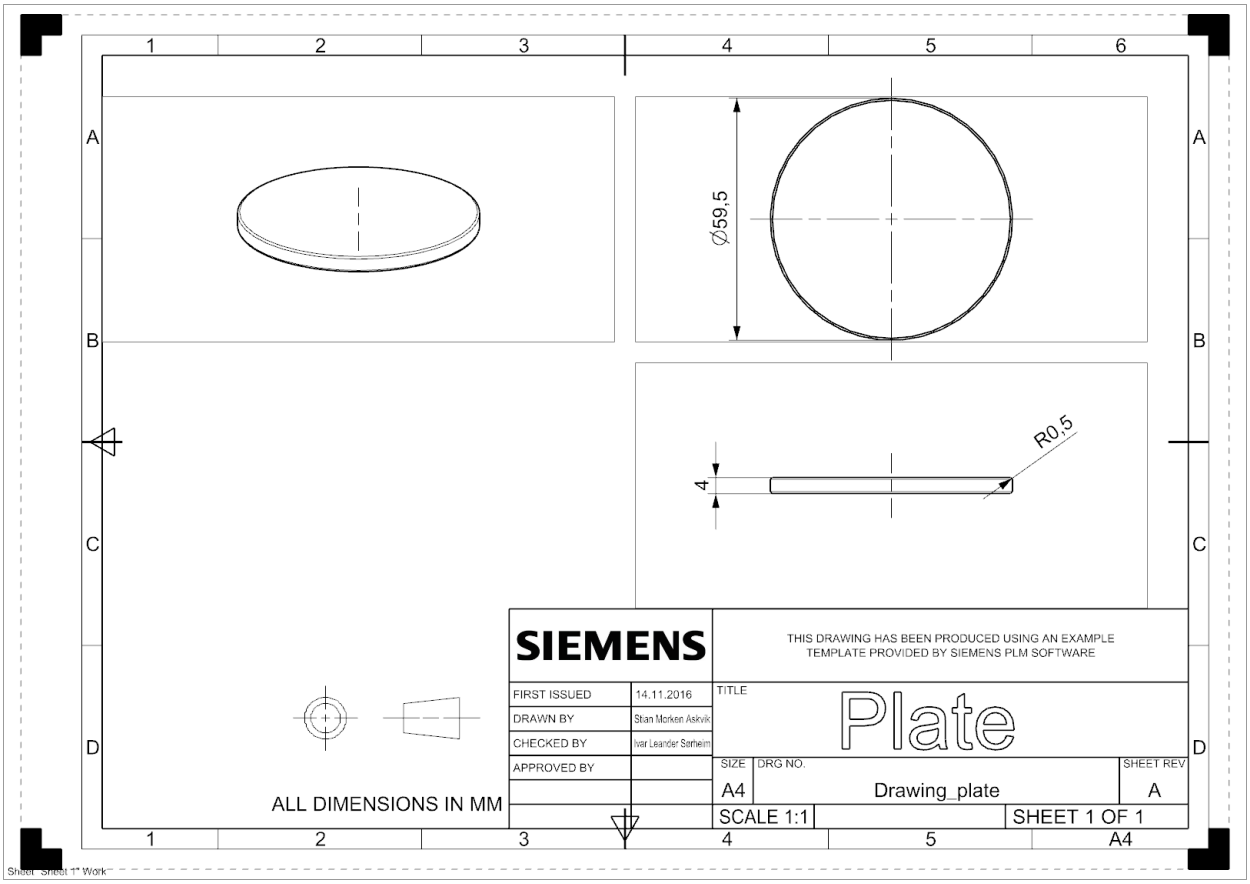

Figure 54: Drawing of moveable disk

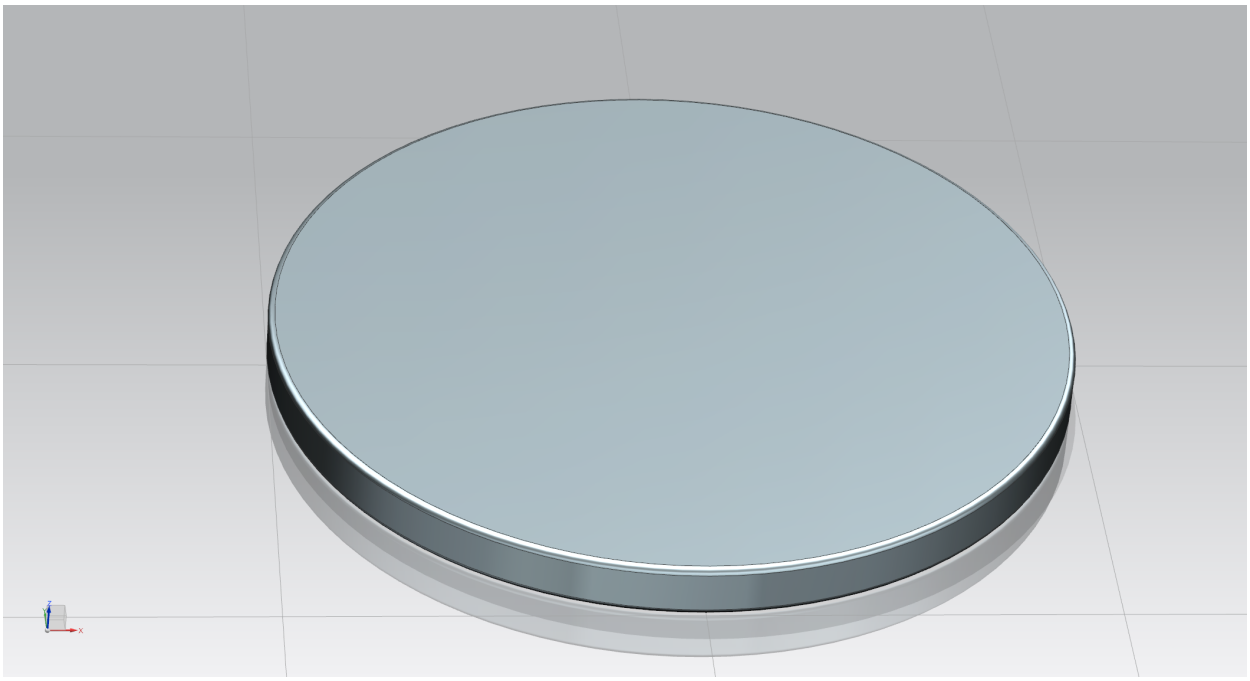

Figure 55: 3D illustration of the plate

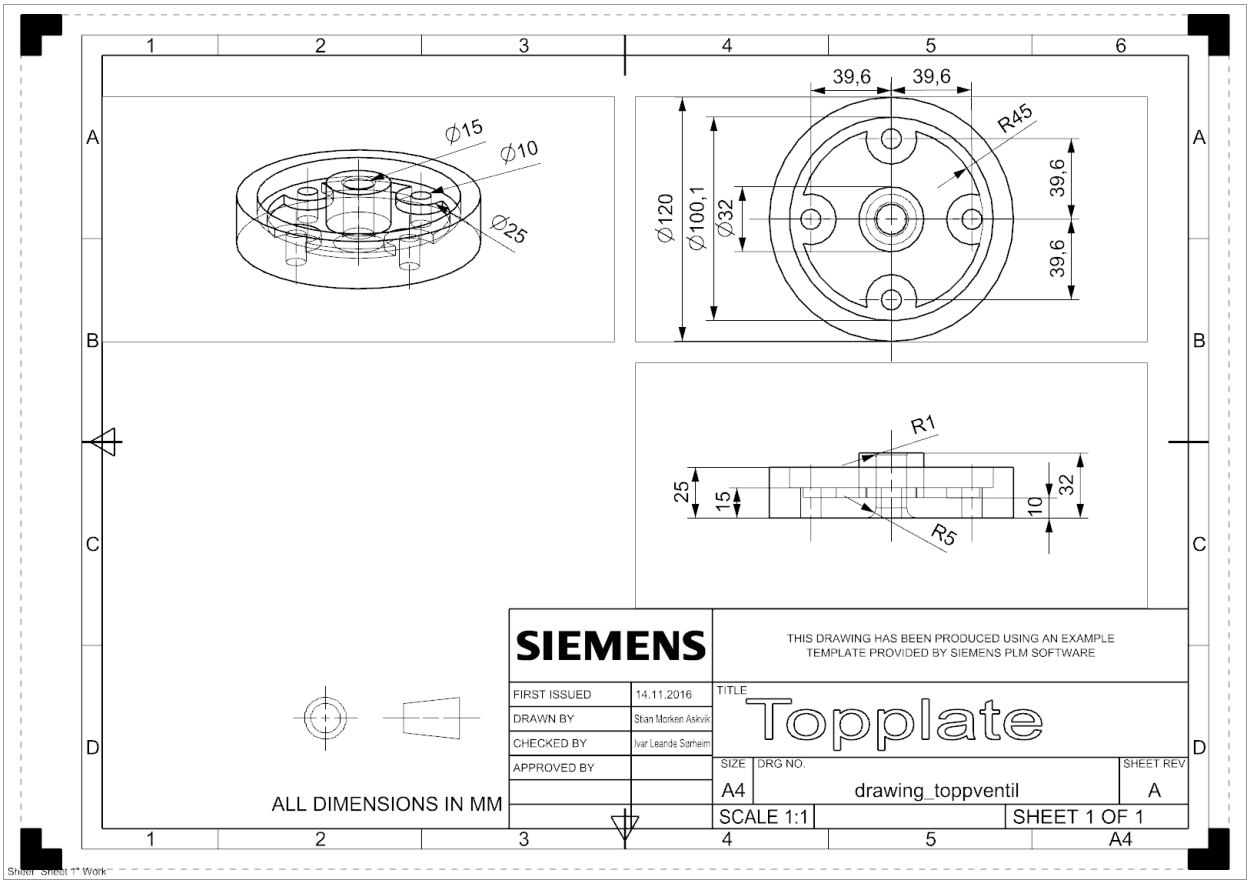

Figure 56: Drawing of top plate

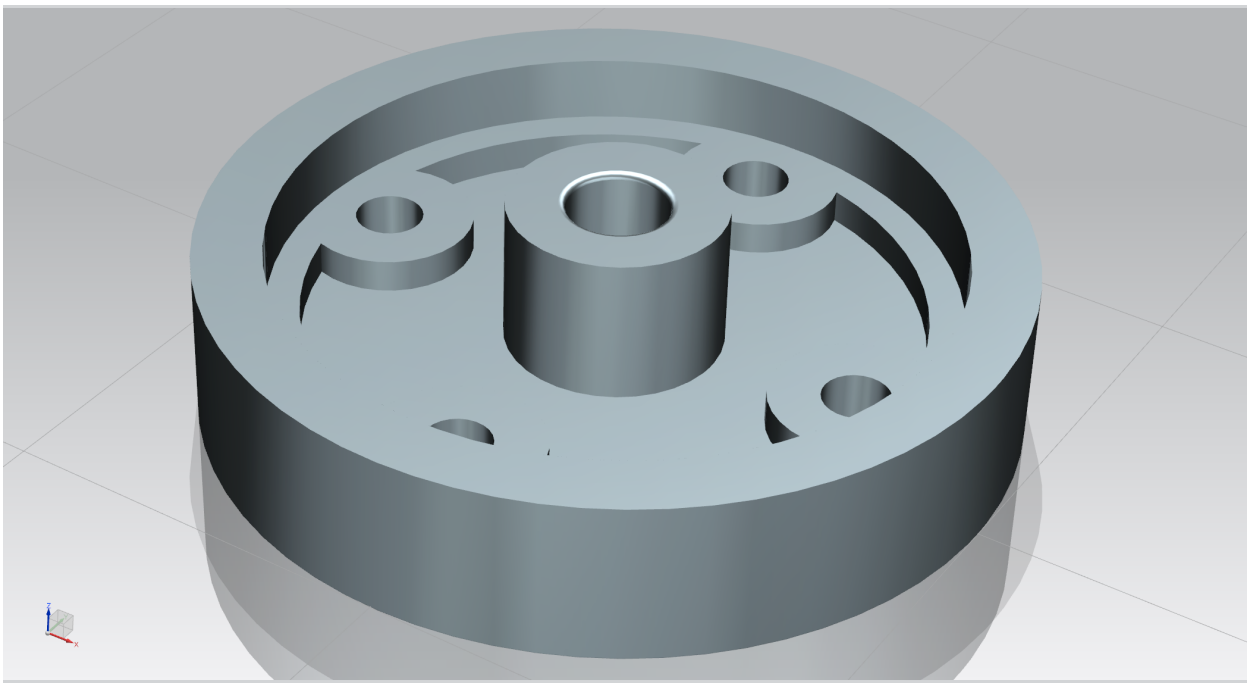

Figure 57: 3D illustration of the top part

A.3 Improved RCP design

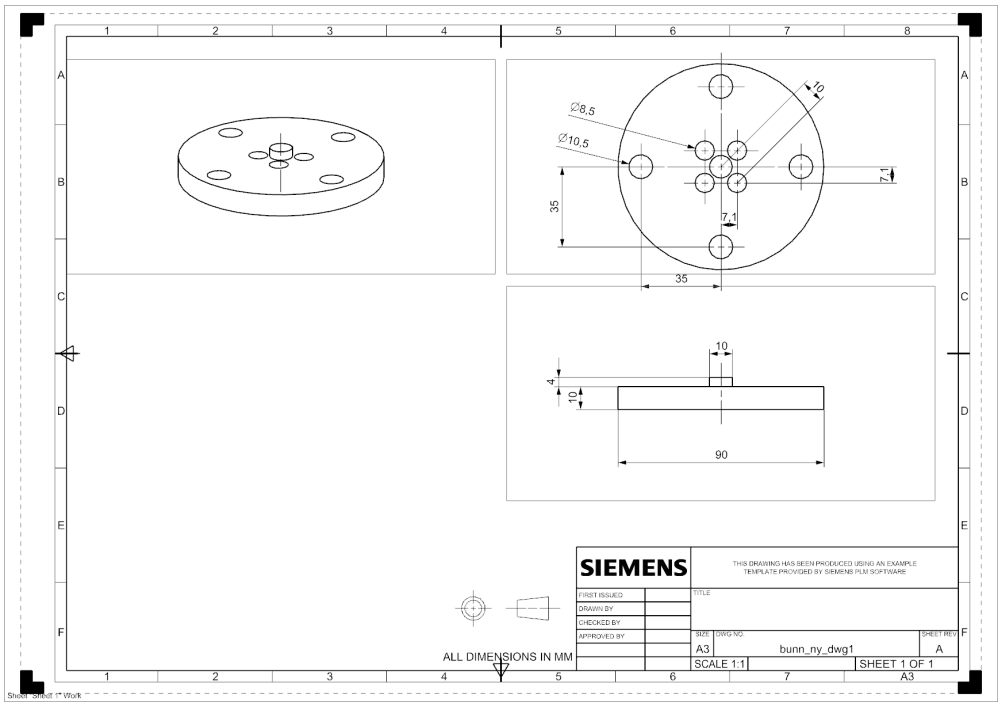

Figure 58: Drawing of the bottom part

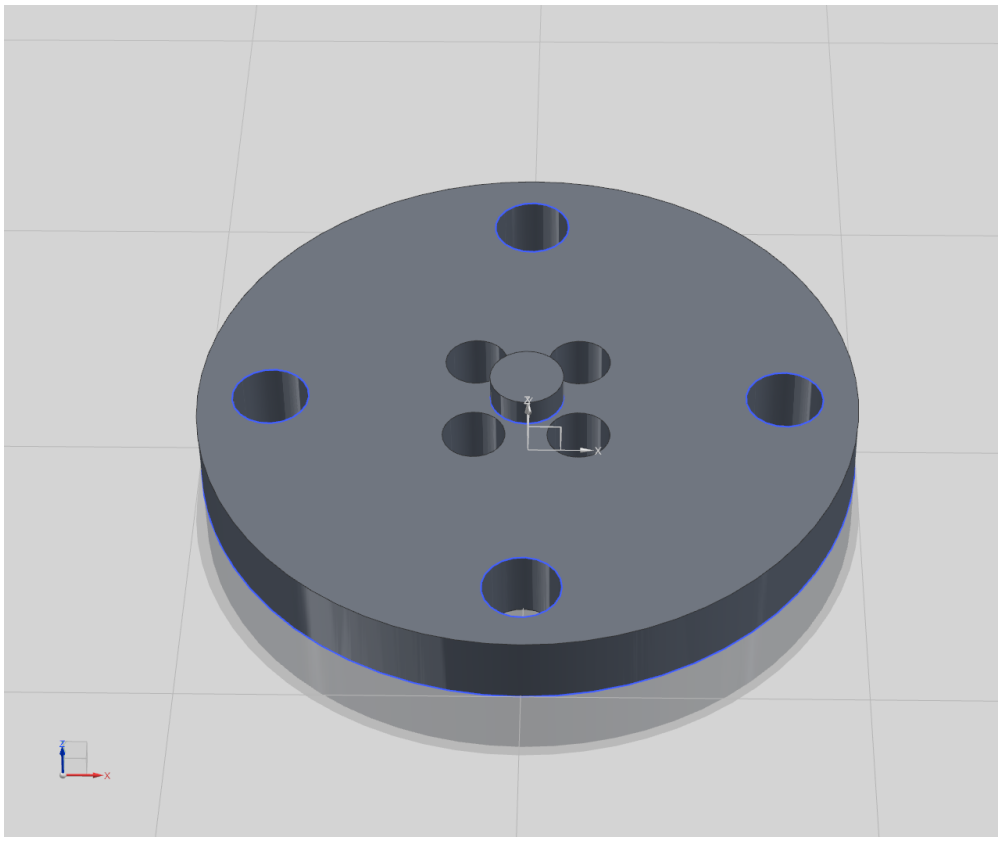

Figure 59: 3D illustration of the bottom part

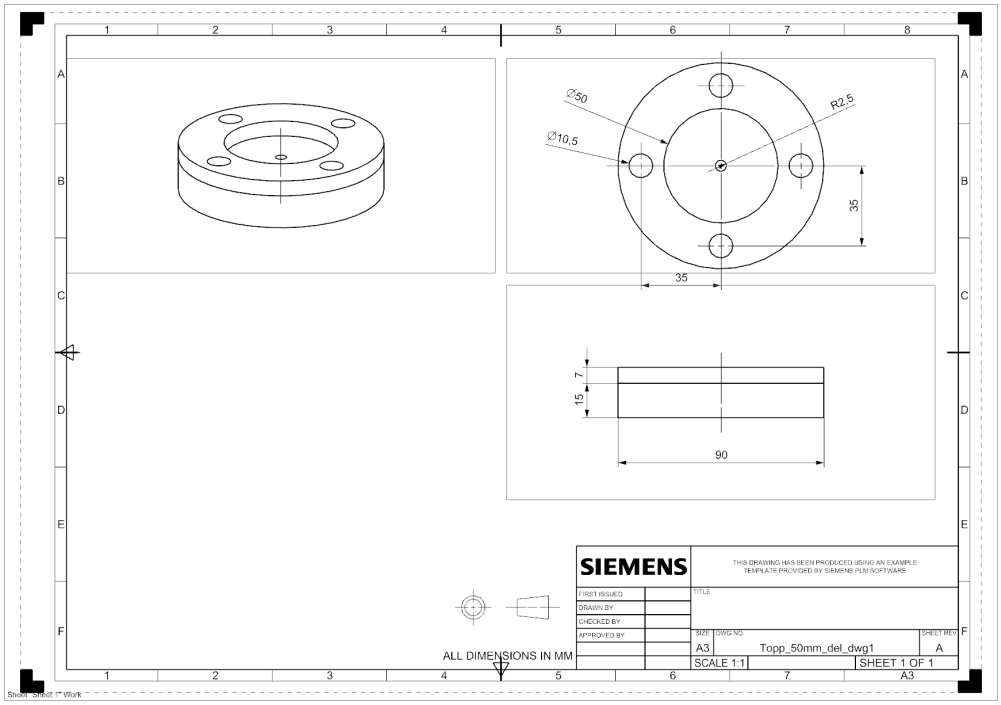

Figure 60: Drawing of the 50mm top part

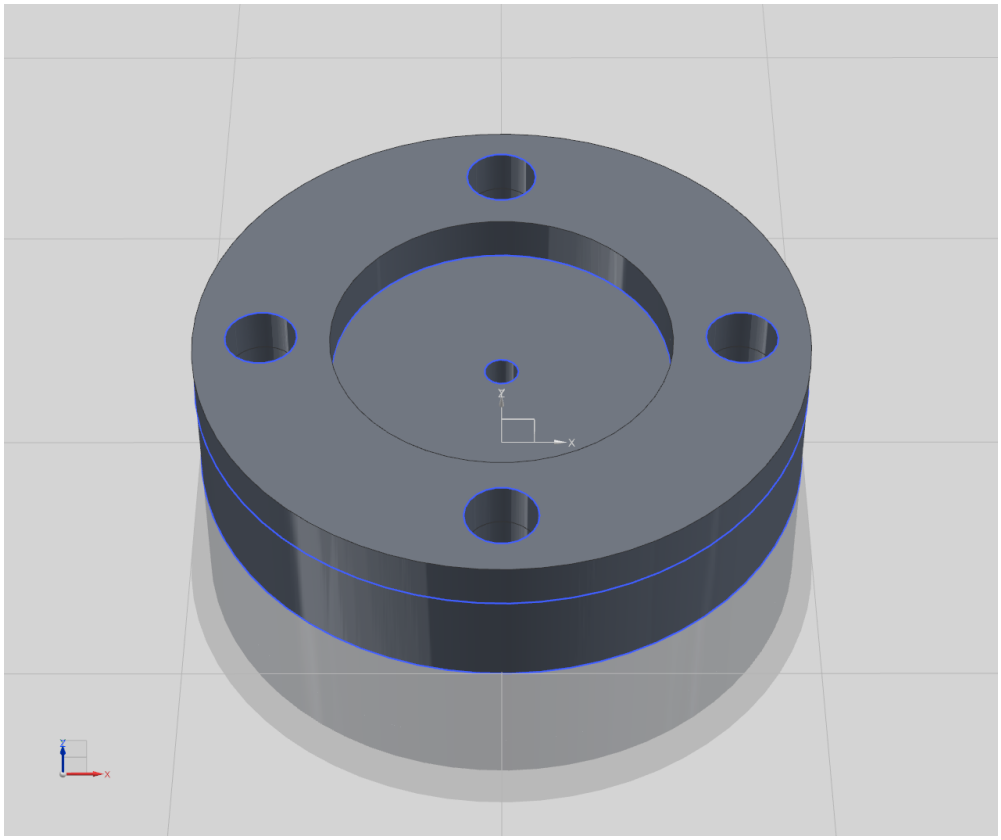

Figure 61: 3D illustration of the 50mm top part

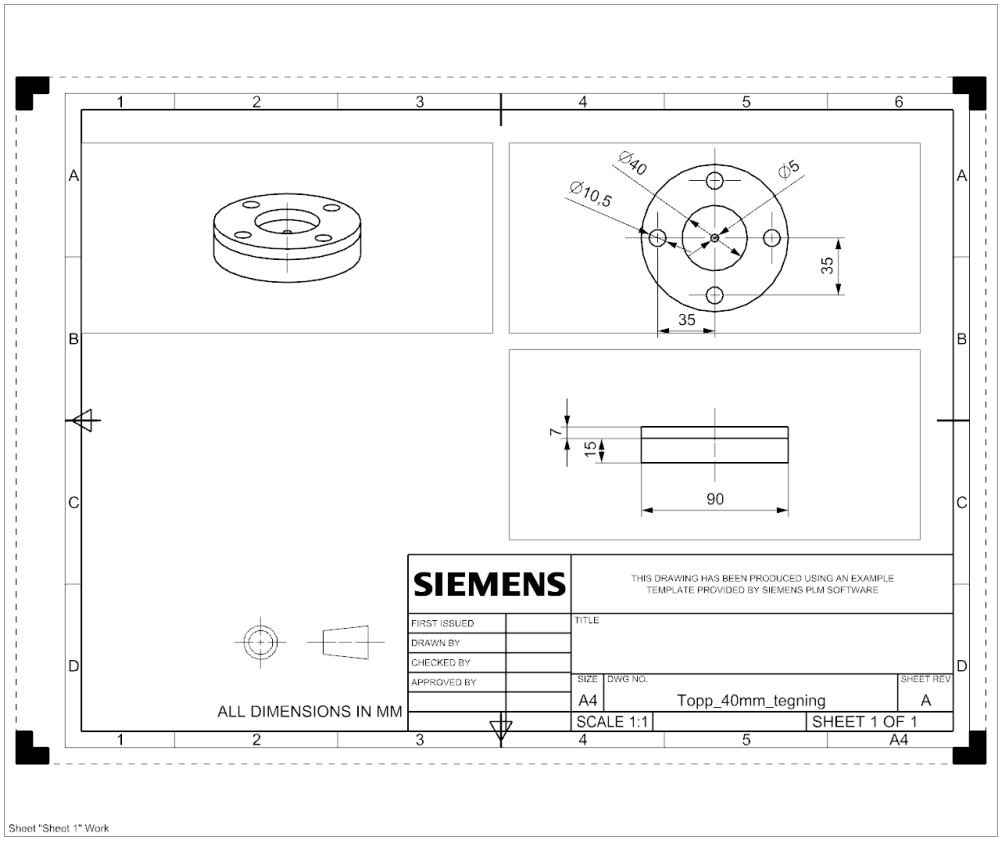

Figure 62: Drawing of the 40mm top part

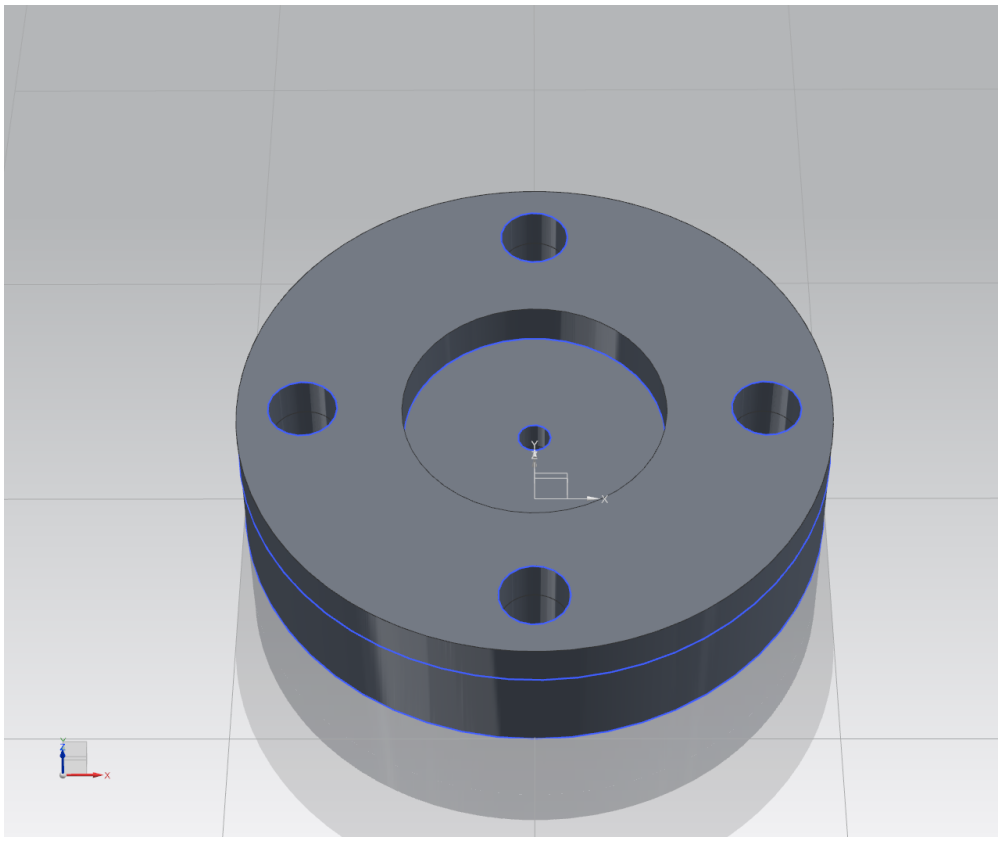

Figure 63: 3D illustration of the 40mm top part

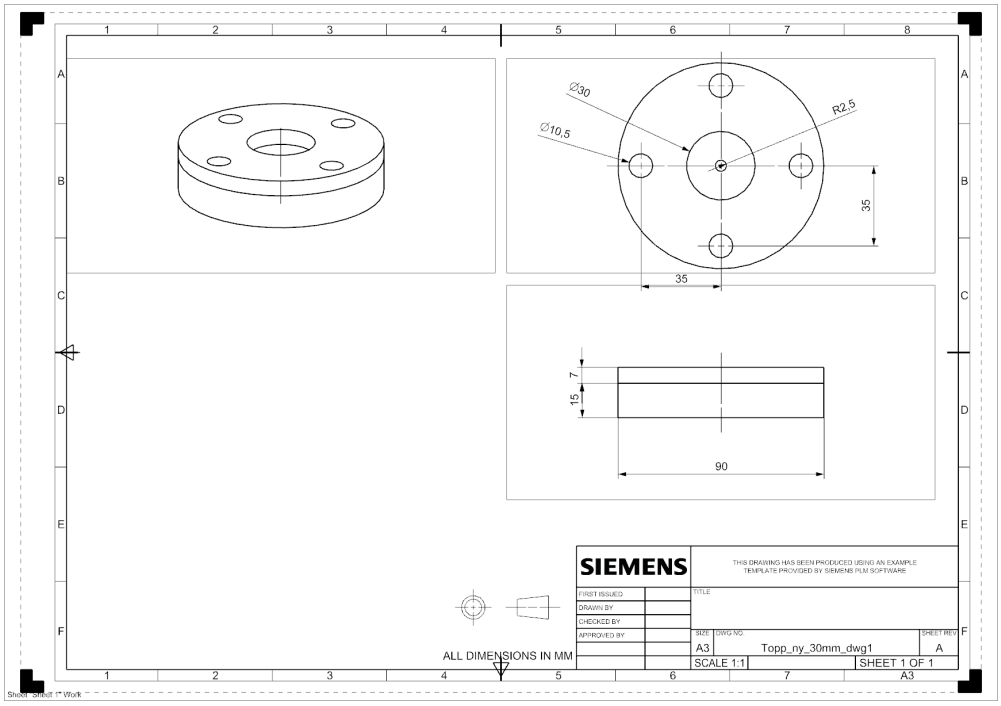

Figure 64: Drawing of the 30mm top part

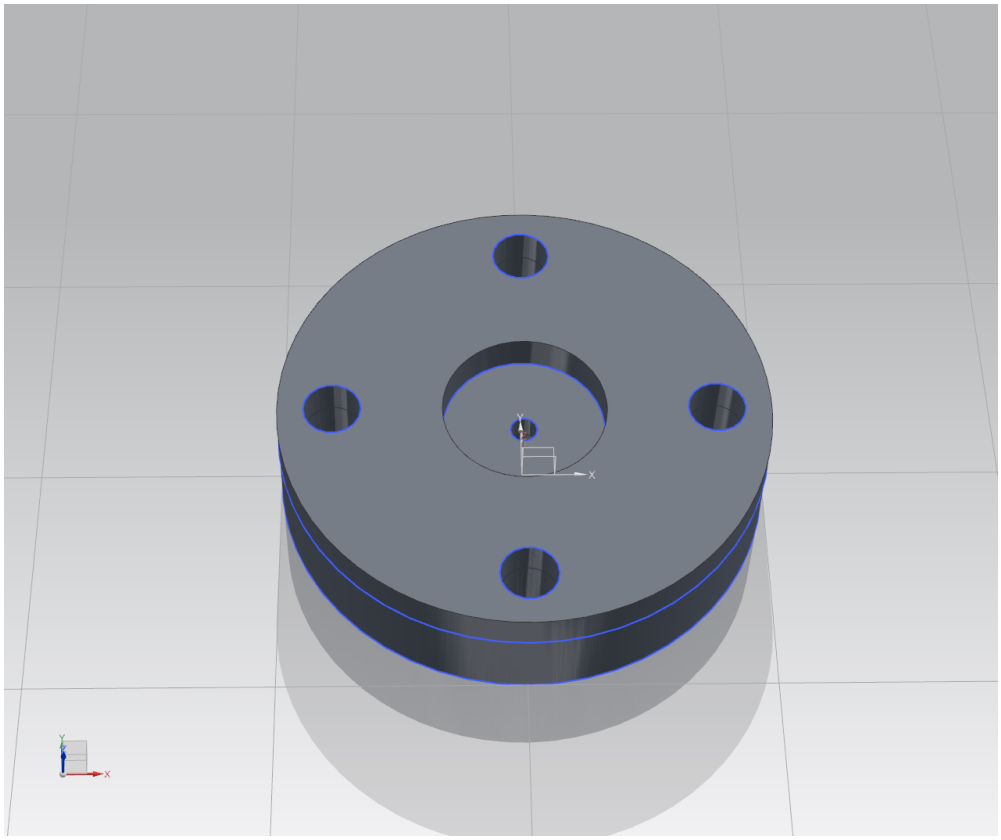

Figure 65: 3D illustration of the 30mm top part